



## Olfactory coding of intra- and interspecific pheromonal messages by the male *Mythimna separata* in North China

Nan-Ji Jiang<sup>a,b</sup>, Rui Tang<sup>a</sup>, Hao Guo<sup>a,b</sup>, Chao Ning<sup>a</sup>, Jian-Cheng Li<sup>c</sup>, Han Wu<sup>a</sup>, Ling-Qiao Huang<sup>a</sup>, Chen-Zhu Wang<sup>a,b,\*</sup>

<sup>a</sup> State Key Laboratory of Integrated Management of Pest Insects and Rodents, Institute of Zoology, Chinese Academy of Sciences, Beijing, 100101, PR China

<sup>b</sup> CAS Center for Excellence in Biotic Interactions, University of Chinese Academy of Sciences, Beijing, 100049, PR China

<sup>c</sup> Integrated Pest Management Center of Hebei Province, Key Laboratory of IPM on Crops in Northern Region of North China, Ministry of Agriculture, Institute of Plant Protection, Hebei Academy of Agricultural and Forestry Sciences, Baoding, 071000, PR China

### ARTICLE INFO

#### Keywords:

*Mythimna separata*  
Pheromone antagonist  
Single sensillum recording  
*In vivo* optical imaging  
Pheromone receptor  
*Xenopus* expression system

### ABSTRACT

Moths often use multi-component pheromones with fixed ratios to keep intraspecific communication and interspecific isolation. Unusually, the Oriental armyworm *Mythimna separata* in North China use only Z11-16:Ald as the essential component of its sex pheromone to find mates. To understand how this species keeps behavioral isolation from other species sharing Z11-16:Ald as a major pheromone component, we study the olfactory coding of intra- and interspecific pheromonal messages in the males of *M. separata*. Firstly, we functionally characterized the long trichoid sensilla in male antennae by single sensillum recording. Two types of sensilla were classified: the A type sensilla responded to Z11-16:Ald and Z9-14:Ald, and the B type sensilla mainly to Z9-14:Ald, and also to Z11-16:Ac, Z11-16:OH, and Z9-16:Ald. Next, we examined the glomerulus responses in the antennal lobes to these compounds by using *in vivo* optical imaging. The results showed that among the three subunits of the macroglomerular complex (MGC), Z11-16:Ald activated the cumulus, Z9-14:Ald activated the dorso-anterior and the cumulus, Z11-16:OH and Z11-16:Ac activated the dorso-anterior and dorso-posterior, respectively. However, Z9-16:Ald activated an ordinary glomerulus. Thirdly, we tested the behavioral responses of the males to these compounds in the wind tunnel. Addition of Z9-14:Ald at the ratio of 1:10 greatly reduced the attractiveness of Z11-16:Ald, addition of Z9-16:Ald or Z11-16:OH at the ratio of 1:1 also had behavioral antagonistic effects, while addition of Z11-16:Ac had no effect on the attractiveness of Z11-16:Ald. Finally, we used antennal transcriptome data and the *Xenopus* expression system to identify the receptor of Z9-14:Ald in *M. separata*. The *Xenopus* oocytes co-expressing MsepOR2 and MsepORco showed a strong response to Z9-14:Ald. Two-color fluorescence *in situ* hybridization validated that the cells expressing MsepOR2 and MsepOR3, tuned to Z9-14:Ald and Z11-16:Ald respectively, were localized in the different sensilla of male antennae. Comparing the sex pheromone communication channel of the related species, our results suggest that the conserved olfactory pathways for behavioral antagonists play a crucial role in behavioral isolation of noctuid species.

### 1. Introduction

Sex pheromones are important chemical signals used by moths to ensure intraspecific sexual communication and interspecific reproductive isolation (Allison and Cardé, 2016; Cardé et al., 1977; Löfstedt and van der Pers, 1985; Roelofs et al., 1974; Touhara and Vossshall, 2009; Wyatt, 2014). Females of most moth species release sex pheromones containing multiple components with specific ratios, which keeps males

to recognize females of the same species accurately (Byer, 2006).

Male moths have sophisticated olfactory systems to recognize the pheromone blends of their own species (Baker et al., 1998; Hansson and Anton, 2000; Leal, 2013). Pheromone components and behavioral antagonists were detected through specific olfactory sensory neurons (OSNs) on the antennae (Baker et al., 2004; Berg et al., 1995). Pheromone receptors (PRs) expressed on the dendrite of OSNs are tuned to the specific compounds (Fleischer et al., 2018). After being transduced, the

\* Corresponding author. State Key Laboratory of Integrated Management of Pest Insects and Rodents, Institute of Zoology, Chinese Academy of Sciences, Beijing, 100101, PR China.

E-mail address: [czwang@ioz.ac.cn](mailto:czwang@ioz.ac.cn) (C.-Z. Wang).

signals are relayed to the macroglomerular complex (MGC) in the antennal lobes (ALs) (Berg et al., 1998; Christensen et al., 1995; Hansson et al., 1991, 1992; Hildebrand and Shepherd, 1997). The MGC is generally formed by 3–4 enlarged glomeruli, where signals of pheromone components and behavioral antagonists are integrated (Baker, 2008; Berg et al., 2005; Hansson et al., 1995; Wu et al., 2015). The outcome of this integration is relayed by the ALs, further integrated with other sensory modalities in the protocerebrum, and finally translated into behavioral responses by sending electrical signals to the muscular system (Hansson and Stensmyr, 2011; Hildebrand and Shepherd, 1997).

Pheromone blends and ratios of components allow more information to be encoded and makes greater discrimination among closely related species. Intriguingly, some species utilize a single compound based pheromone to find their partners. (*E,Z*)-10,12-hexadecadien-1-ol, (*E,E*)-8,10-dodecadienol, and Z-7,8-epoxy-2-methyloctadecane are identified as the single pheromone compounds of the silk worm *Bombyx mori*, the coding moth *Cydia pomonella*, and the gypsy moth *Lymantria dispar*, respectively (Bierl et al., 1970; Butenandt et al., 1962; McDonough et al., 1995; Witzgall et al., 2008). These chemicals are quite unique to these species, thus isolating them from other species. However, the Oriental armyworm, *Mythimna separata* in the North China uses (*Z*)-11-hexadecenal (*Z*11-16:Ald) as its essential pheromone component, and the single compound could induces the entire sequence of male sexual behaviors in the wind tunnel (Jiang et al., 2019). *Z*11-16:Ald, as a broadly employed type I pheromone compound, is also used by almost all of *Heliothis* and *Helicoverpa* species as the principal pheromone component. For example, *Heliothis virescens* uses *Z*11-16:Ald and (*Z*)-9-tetradecenal (*Z*9-14:Ald) as its principal pheromone components at a ratio of 16:1 (Klun et al., 1980; Roelofs et al., 1974; Tumlinson et al., 1975); *Helicoverpa armigera* use *Z*11-16:Ald and (*Z*)-9-hexadecenal (*Z*9-16:Ald) as its principal pheromone components at a ratio of around 10:1 (Nesbitt et al., 1979; Wang et al., 2005), and *Z*9-14:Ald as an agonist in small amounts (0.3%) but an antagonist in higher amounts (1% and above) (Gothilf et al., 1978; Rothschild, 1978; Wu et al., 2015; Zhang et al., 2012). How males of *M. separata* in North China detect its own sex pheromone and keep behavioral isolation from those species sharing *Z*11-16:Ald as a major pheromone component is still unclear. Dissecting the structure of pheromone communication channels is not only helpful to understand reproductive isolation among closely related species, but also particularly important in formulating pheromone-based lures for pest monitoring and control.

The peripheral coding of the sex pheromone in *M. separata* in North China is poorly investigated although many olfaction related genes have been identified through transcriptome analysis (Bian et al., 2017; Chang et al., 2017; Du et al., 2018; He et al., 2017; Liu et al., 2017). Recently, we examined its sex pheromone communication and found that *Z*11-16:Ald is specifically tuned by MsepOR3 and elicits EAG responses of the antennae, and then activates the cumulus of the MGC in male ALs (Jiang et al., 2019), which is very similar to that of *Heliothis* and *Helicoverpa* species using *Z*11-16:Ald as a major pheromone component. The pheromone communication systems of several *Heliothis* and *Helicoverpa* species have been extensively studied (Hillier and Baker, 2016). The underlying circuitry of the pheromone olfactory systems is quite similar across this group of species. Three functional types of sensilla on the male antennae of *Heliothis* and *Helicoverpa* species can be classified (Baker et al., 2004; Berg et al., 1995). The A type of sensilla contains an OSN expressing OR13, which is specifically tuned to the major pheromone component *Z*11-16:Ald, and projects to the cumulus (CU) of MGC (Baker et al., 2004; Berg et al., 1998; Grosse-Wilde et al., 2007; Krieger et al., 2004; Liu et al., 2013; Wang et al., 2011; Wu et al., 2013, 2015; Zhang et al., 2010). The B type of sensilla contains an OSN responding to (*Z*)-9-tetradecenal (*Z*9-14:Ald), and the C type of sensilla contains two neurons, one mainly responding to the secondary pheromone component and another to behavioral antagonists, and the axons of these neurons are sent to the other two or three glomeruli of MGC (Baker et al., 2004; Berg et al., 1998, 2005; Wu et al., 2013, 2015; Xu et al., 2016).

Some of related PRs have also been functionally identified (Jiang et al., 2014; Liu et al., 2013; Wang et al., 2011; Yang et al., 2017).

To understand how *M. separata* keeps behavioral isolation from other species sharing *Z*11-16:Ald as a major pheromone component, we study the olfactory coding of intra- and interspecific pheromonal messages in the males of *M. separata*. Firstly, we investigated the electrophysiological responses of long trichoid sensilla in male antennae to the pheromonal compounds of *M. separata* and *Heliothis/Helicoverpa* species by single sensillum recording (SSR), and then examined the neural representation of the reactive compounds in glomeruli of ALs by *in vivo* optical imaging, and thirdly tested the behavioral responses of the males to these compounds in the wind tunnel. Finally, we use antennal transcriptome data, the *Xenopus* expression system and two-electrode voltage-clamp, and two-color fluorescence *in situ* hybridization to identify the PR tuned to *Z*9-14:Ald in *M. separata*.

## 2. Results

### 2.1. Functional characterization of long trichoid sensilla of male *M. separata*

To characterize the long trichoid sensilla of male *M. separata*, pheromone gland compounds presented in *M. separata* and its sympatric species *H. armigera* and *H. assulta* (Nesbitt et al., 1979; Wang et al., 2005; Zhang et al., 2012) were utilized in SSR experiments. The sensilla were classified into two types (A and B types) based on their response profiles. The A type sensilla had electrophysiological responses to both *Z*11-16:Ald and *Z*9-14:Ald dose-dependently (Fig. 1A and B). However, the response threshold dosage of *Z*11-16:Ald (10 µg) is lower than that of *Z*9-14:Ald (100 µg), and the firing rate induced by *Z*11-16:Ald was much higher than that by *Z*9-14:Ald (Fig. 1A and B). To verify if the responses to *Z*11-16:Ald and *Z*9-14:Ald were from one or two separate neurons, we further compared the responses to the mixture of *Z*11-16:Ald and *Z*9-14:Ald with the ratio of 1:1 and the single compounds at the dosage of 100 µg. The results show that the amplitudes of the spikes elicited by the mixtures were uniform (Fig. 2A). The firing rate for the mixture of 50 µg *Z*11-16:Ald and 50 µg *Z*9-14:Ald was much lower than that for 100 µg *Z*11-16:Ald, which then had no difference with that for the mixture of 100 µg *Z*11-16:Ald and 100 µg *Z*9-14:Ald, indicating *Z*11-16:Ald played a dominant role in the mixtures (Fig. 2B). Comparing with the A type sensilla, the B type sensilla had a more expanded response profile. They had a strong response to *Z*9-14:Ald, and also responded to (*Z*)-11-hexadecenol (*Z*11-16:OH), (*Z*)-11-hexadecenyl acetate (*Z*11-16:Ac), and (*Z*)-9-hexadecenal (*Z*9-16:Ald) (Fig. 1C). The dose-response curves show that the B type sensilla were more sensitive to *Z*9-14:Ald than A type sensilla, and the response threshold dosage is 10 µg (Fig. 1D). Among the recorded long trichoid sensilla in the male antennae, the percentages of A and B type sensilla were about 66% and 34%, respectively.

### 2.2. Neural representation of male *M. separata* glomeruli to *Z*9-14:Ald

The morphological atlas of antennal lobes (ALs) of male *M. separata* has been built in the previous study (Jiang et al., 2019). The macroglomerular complex (MGC) of male *M. separata* consists of three sub-units: the cumulus (CU); the dorso-anterior (DA) and the dorso-posterior (DP). According to the AL atlas and *in vivo* optical imaging data, we have determined that the essential pheromone component *Z*11-16:Ald activated the CU, the largest subunit of MGC (Jiang et al., 2019). With the same methods, in this study we identified the glomeruli activated by *Z*9-14:Ald, *Z*11-16:OH, *Z*11-16:Ac, and *Z*9-16:Ald (Fig. 3).

Based on the overlapping of the fake color graphs with the grey graph, we proved that *Z*11-16:Ald specifically activated the CU, and found that *Z*9-14:Ald activated DA and CU of MGC, and *Z*11-16:OH, *Z*11-16:Ac, and *Z*9-16:Ald activated DA, DP, and one ordinary glomerulus called OG1, respectively (Fig. 3A and B). We calculated the relative response area of each compound, and the results showed that the area of

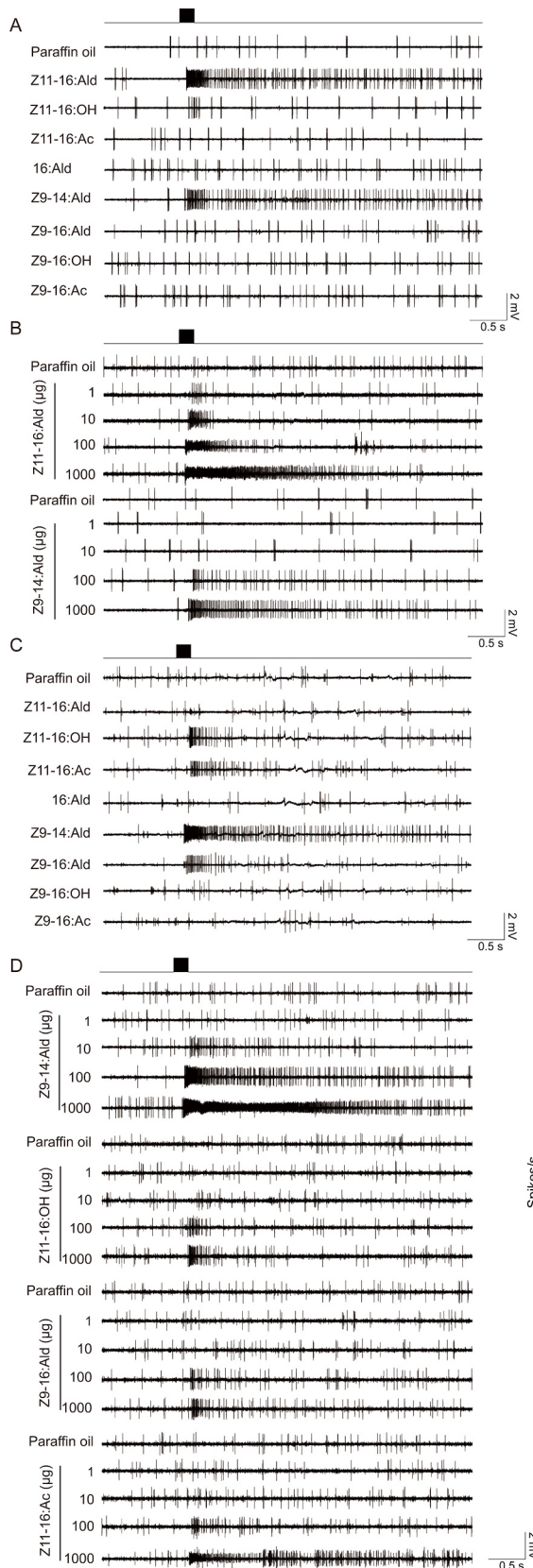
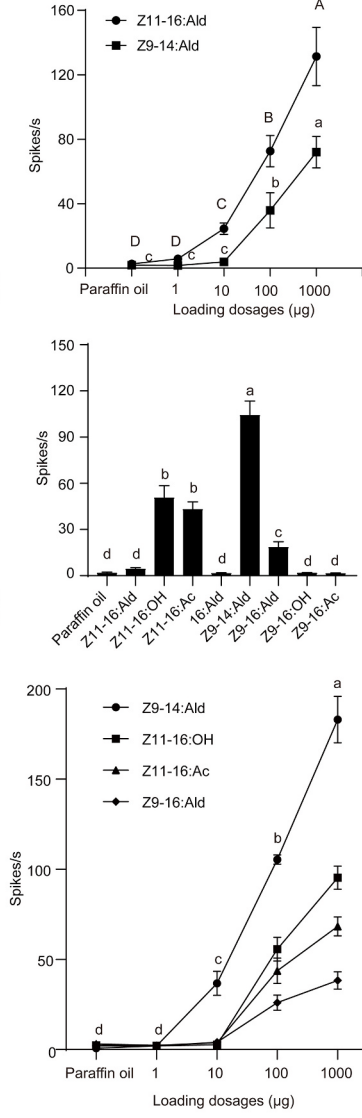


**Fig. 1.** The electrophysiological responses of two types of long trichoid sensilla in antennae of male *M. separata* to intra- and interspecific pheromonal compounds. (A) The responding profile of A type sensilla ( $N = 63$ ); (B) Dose-response curves of A type sensilla to Z11-16:Ald ( $N = 11$ ) and Z9-14:Ald ( $N = 5$ ); (C) The responding profile of B type sensilla ( $N = 28$ ); (D) Dose-response curves of B type sensilla to Z9-14:Ald, Z11-16:OH, Z11-16:Ac and Z9-16:Ald ( $N = 3$  for each). The left panel shows representative traces, and the black bar indicates the stimulus duration. The right panel shows the firing rates, the data are presented as mean  $\pm$  SE, and the values with different letters are significantly different (ANOVA & Tukey HSD multiple comparison,  $P < 0.05$ ).



Z9-14:Ald overlapped with the area of Z11-16:Ald and the area of Z11-16:OH (Fig. 3B). The  $\Delta F/F$  values of the four glomeruli of male ALs showed that the activity of CU elicited by Z11-16:Ald was much higher than that by Z9-14:Ald, the activity of DA elicited by Z9-14:Ald was

higher than that by Z11-16:OH, at the same dosage (Fig. 3C). The activities of DP and OG1 were specifically elicited by Z11-16:Ac and Z9-16:Ald, respectively (Fig. 3C).

We also tested the response pattern of ALs elicited by the mixtures of

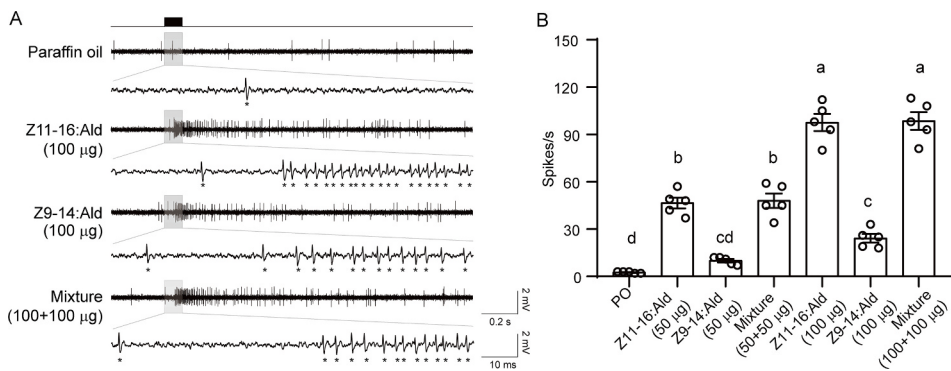


**Fig. 2. Responses of A type sensilla in antennae of male *M. separata* to Z11-16:Ald, Z9-14:Ald and their mixtures. (A)** Spikes of one A type sensillum representative. The black bar shows the stimulus duration. Up: the firing trace in 2 s; Below: the amplification of the grey part, the star represents the spikes from one olfactory sensory neuron. (B) The firing rates (mean  $\pm$  SE, N = 5). PO: paraffin oil. Columns with different letters are significantly different (ANOVA & Tukey HSD multiple comparison, P < 0.05).

Z11-16:Ald and Z9-14:Ald, which was compared with the patterns elicited by single compounds. Three mixtures, Mix 1, Mix 2 and Mix 3, are Z11-16:Ald mixed with Z9-14:Ald at the ratios of 100:1, 10:1, and 1:1, respectively. The results indicate that Mix 1 mainly activated the CU, while the Mix 2 and Mix 3 activated both CU and DA, indicating that addition of Z9-14:Ald in the mixtures only elicited the activity of DA with no effect on the CU activity (Fig. 3A and C).

To determine which subunit was more sensitive to Z9-14:Ald in the MGC, we further investigated the dose-response curves of CU and DA to Z9-14:Ald. We found that DA was the first activated by Z9-14:Ald at a dosage of 10 µg, and then both DA and CU were activated when the dosage is getting higher ( $\geq 100$  µg) (Fig. 4).

### 2.3. Z9-14:Ald as a strong behavioral antagonist of *M. separata* males

Considering Z9-14:Ald was sensed by so many long trichoid sensilla on the male antennae and could activate both CU and DA in male ALs, we further examined if it exists in the sex pheromone gland of the *M. separata* female. By using GC-MS we proved that Z9-14:Ald was not presented in the pheromone gland extracts of virgin females from 1-day to 7-day-old and of the mated females. Z9-16:Ald was also absent in the pheromone gland extracts, but Z11-16:Ald, Z11-16:OH, and Z11-16:Ac were detected there (Fig. S1).

We then tested the behavioral effect of Z9-14:Ald and other three compounds, Z9-16:Ald, Z11-16:OH and Z11-16:Ac, on the male attractiveness of Z11-16:Ald in a wind tunnel. Firstly, we used Z11-16:Ald at a dosage of 10 ng (similar to 1 female equivalent) in the related lures when other compound was mixed in at high ratios. The results showed that the lures of pheromone gland extracts or single Z11-16:Ald induced male moths exhibit the full sequences of pre-mating behaviors, flight, upwind, closing, landing, and even trying to mate (Fig. 5A). When Z9-14:Ald was added to the lures of pheromone gland extracts or single Z11-16:Ald at the ratio of 1:10, the male moths only showed flight, upwind and closing, but no landing and mating (Fig. 5A). When Z9-14:Ald was mixed with Z11-16:Ald at the ratio of 1:1, the male moths still showed flight and upwind, but no closing (Fig. 5A). Addition of Z9-16:Ald or Z11-16:OH to the lure of Z11-16:Ald at the ratio of 1:10 and addition of Z11-16:Ac at the ratio of 1:1 had no effect on the attractiveness of Z11-16:Ald (Fig. 5A). However, addition of Z9-16:Ald or Z11-16:OH to the lure of Z11-16:Ald at the ratio of 1:1 showed antagonistic effects similar to that of Z9-14:Ald (Fig. 5A).

To further determine behavioral effects of Z9-14:Ald at even lower ratios on the attractiveness of Z11-16:Ald, we used Z11-16:Ald at a dosage of 1 µg in the related lures when Z9-14:Ald or Z9-16:Ald was mixed in. When Z9-14:Ald was mixed with Z11-16:Ald at the ratio of 1:100, the upwind flight males were significantly decreased and only 3% of males got close to lures (Fig. 5B). We also tested the pheromone lure of Z9-16:Ald mixed with Z11-16:Ald at the ratio of 3:100, the results showed that 37% of males got close to the lure and only 13% of males landed (Fig. 5B). In summary, Z9-14:Ald acts as a strong behavioral

antagonist in the pheromone communication of *M. separata*, and Z9-16:Ald is also an antagonist but the effect is weaker than Z9-14:Ald.

### 2.4. Determination of the pheromone receptor of Z9-14:Ald

Based on the transcriptome sequencing data of male and female antennae, we conducted neighbor-joining analysis with data of other noctuid species and identified six putative PRs and olfactory co-receptor (ORco) of *M. separata*, MsepOR1, MsepOR2, MsepOR3, MsepOR4, MsepOR5, MsepOR6, and MsepORco (GenBank accession numbers: MK414778, MH717242, MH717241, MK414779, MK414780, MK414781, and MH717243) (Fig. 6). Though the PRALINE multiple sequence alignment (Simossis et al., 2003, 2005) of all together with the previously reported PRs of other species in Noctuidae, we found that MsepOR2 is conserved in amino acid sequences with SinfOR21, HassOR16, HvirOR6, and HarmOR14b (Fig. S2). MsepOR2 is a male-bias expressed PR in *M. separata* antennae (Jiang et al., 2019), sharing 78.9%, 70.6%, 67.2%, and 55.3% identity with SinfOR21, HassOR16, HvirOR6, and HarmOR14b in the amino acid sequence. SinfOR21 is reported to be tuned to Z11-16:OH (Zhang et al., 2014), while HassOR16, HvirOR6, and HarmOR14b are all reported to be tuned to Z9-14:Ald (Jiang et al., 2014; Liu et al., 2013; Wang et al., 2011; Yang et al., 2017). Therefore, we predicted that MsepOR2 could be the PR tuned to Z9-14:Ald or Z11-16:OH. To test this, we co-expressed MsepOR2 with MsepORco in *Xenopus* oocytes, and used two-electrode voltage-clamp recording to test the oocyte response to a range of pheromone components of noctuid species and related compounds. The results showed that the oocytes co-expressing MsepOR2 and MsepORco evoked a dose-dependent response to Z9-14:Ald, and a weak response to Z11-16:OH (Fig. 7).

### 2.5. Spatial organizations of MsepOR2 and MsepOR3 in male antennae

In *M. separata* males, MsepOR3 has been deorphanized to the sex pheromone Z11-16:Ald (Jiang et al., 2019) and MsepOR2 is mainly tuned to Z9-14:Ald (Fig. 7), while the A type sensilla are responsive to Z11-16:Ald and Z9-14:Ald (Fig. 1A and B), and the B type sensilla are responsive to Z9-14:Ald and three other compounds (Fig. 1C and D). Therefore, we speculate that MsepOR3 is expressed in the A type sensilla, and MsepOR2 could be expressed in A or B type sensilla. To test if the cell expressing MsepOR3 and the cell expressing MsepOR2 are co-localized in the same sensilla, we used two-color *in situ* hybridization to analyze the spatial expression of MsepOR3 (biotin-labeled, green) and MsepOR2 (digoxigenin-labeled, red) in the male antennae. Results show that the cells expressing MsepOR2 and the cells expressing MsepOR3 beneath the cuticle are separately localized in different sensilla (Fig. 8), suggesting that MsepOR2 is expressed in the B type sensilla.

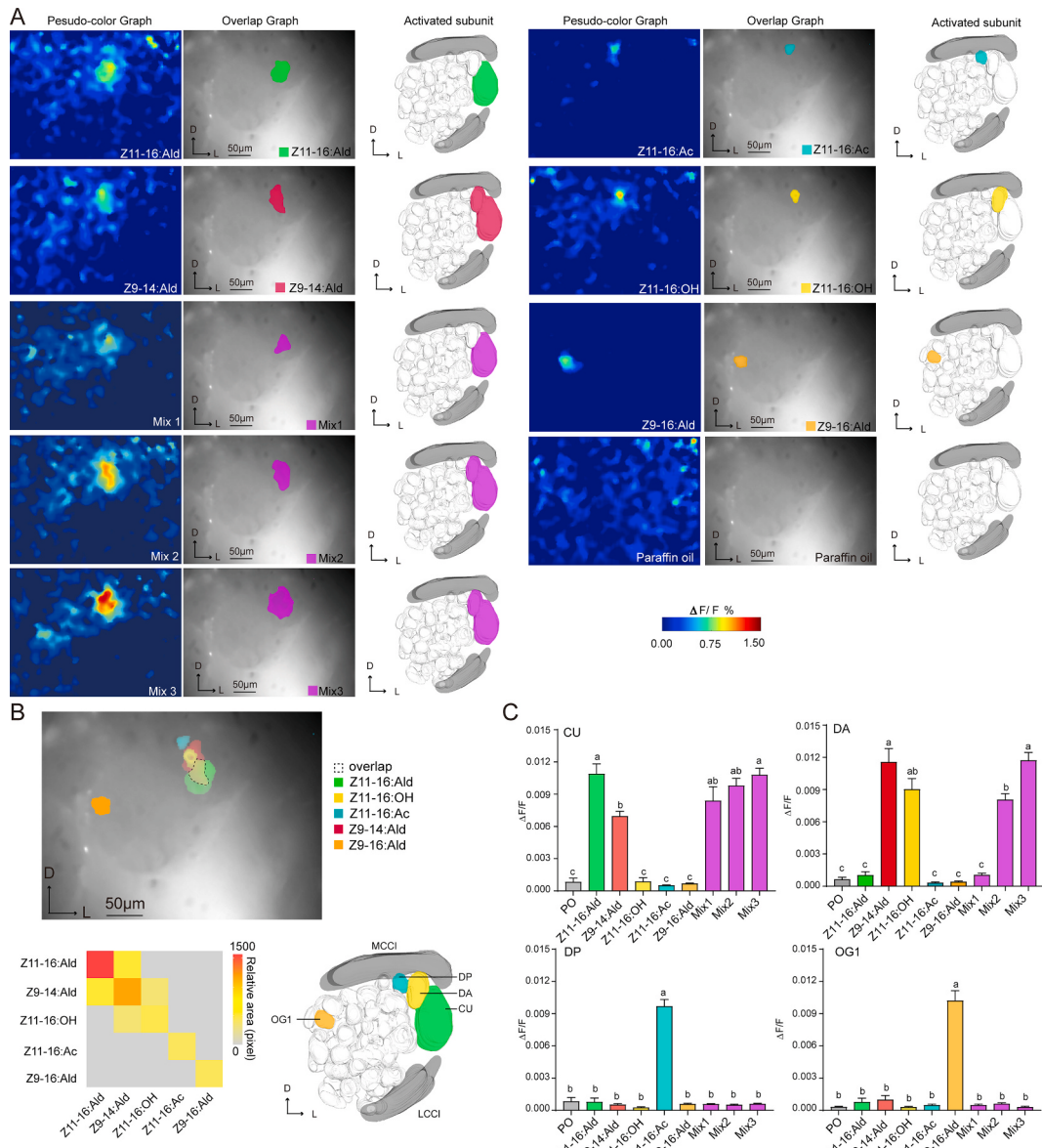


**Fig. 3. The glomerular responses in the antennal lobe (AL) of male *M. separata* to intra- and interspecific pheromonal compounds.** Single compounds: 100 µg; Mix 1: Z11-16:Ald 100 µg + Z9-14:Ald 1 µg; Mix 2: Z11-16:Ald 100 µg + Z9-14:Ald 10 µg; Mix 3: Z11-16:Ald 100 µg + Z9-14:Ald 100 µg. (A) The pseudo-color graph (left) shows the spatial response pattern in the AL; the grey graph (middle) shows the activated pattern superimposed on the grey-scale image of the AL indicating the relative position of the response in the AL; the 3D-structure (right) shows the activated glomerulus in the AL. D: dorsal; L: lateral. (B) The activated patterns of different compounds superimposed on the grey scale image of the AL (up), the heat map of averaged relative overlap area (pixel) of glomeruli activated by the compounds ( $N = 11$ ) (down left) and the four glomeruli activated by the compounds (down right). MCCL: medial cell cluster. LCCI: lateral cell cluster. CU: cumulus. DA: dorso-anterior. DP: dorso-posterior. OG1: ordinary glomerulus 1. (C) Response activities of four glomeruli to the compounds and mixtures. PO: paraffin oil. All data are presented as mean  $\pm$  SE ( $N = 11$ ). Columns with different letters are significantly different (ANOVA & Tukey HSD multiple comparison,  $P < 0.05$ ).

### 3. Discussion

To keep the intra-specific communication and avoid the inter-specific hybridization, most moth species use multi-component sex pheromones with a specific ratio to find mates. It is particular that *M. separata* in North China just has one essential component, Z11-16:Ald for pheromone communication (Jiang et al., 2019). However, simple pheromone doesn't mean simple pheromone communication. Synthesizing all the results in this study, we can draw the outline of at least two principal olfactory coding pathways in the pheromone detection system of *M. separata* males. One pathway is mainly coding for the essential pheromone component Z11-16:Ald. MsepOR3 tuned primarily to Z11-16:Ald is expressed in one OSN within each of the most abundant A type sensilla, and the axons of these neurons project to the CU of the

MGC in male ALs. Another pathway is mainly coding for the behavioral antagonist Z9-14:Ald. MsepOR2 tuned to Z9-14:Ald is expressed in one OSN housed within each of the B type sensilla, and the axons of these neurons project to the DA of the MGC in male ALs. Anyway, other pathways coding for Z11-16:OH, Z11-16:Ac, and Z9-16:Ald related to the B type sensilla also play a part in the system.

#### 3.1. The organization of the pheromone detection system in *M. separata*

Following the central dogma of olfactory biology: One population of OSNs expressing a single OR converges upon one unique olfactory glomerulus (Fishilevich and Vosshall, 2005), we can figure out the main pheromone detection system in males of *M. separata* based on the results of this study (Fig. 9). Two types of sensilla involved in the pheromone

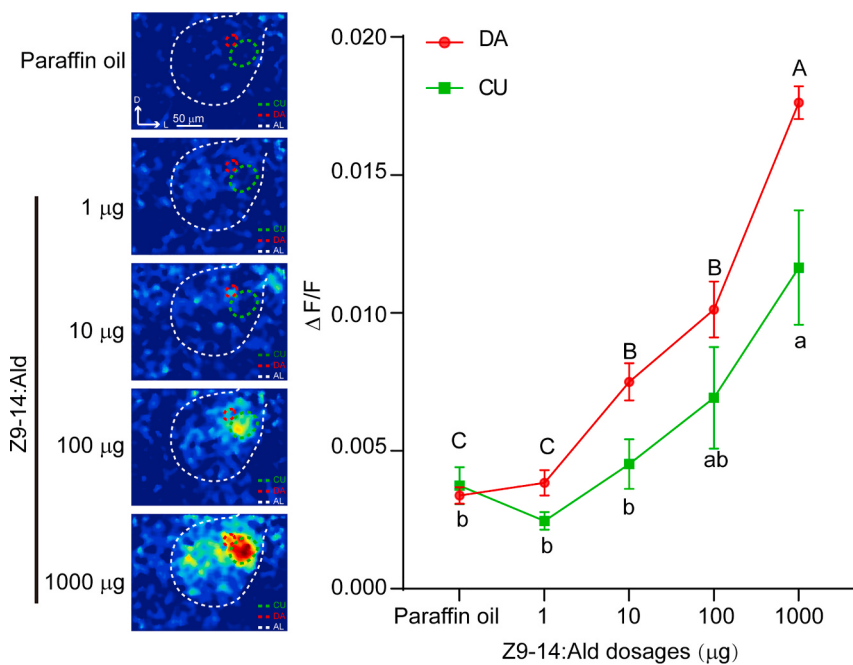


**Fig. 4. The dose-responses of glomeruli in the antennal lobe of male *M. separata* to Z9-14:Ald.** The left panel is the spatial response pattern in the antennal lobe. Paraffin oil as the control. AL: antennal lobe; CU: cumulus; DA: dorso-anterior. D: dorsal; L: lateral. The right is the dose-response curves of CU and DA. The data are presented as mean  $\pm$  SE (N = 5). The values with different letters are significantly different (ANOVA & Tukey HSD multiple comparison,  $P < 0.05$ ).

detection of *M. separata* were identified: the A type sensilla respond to Z11-16:Ald and Z9-14:Ald, and the B type sensilla respond to Z9-14:Ald, Z11-16:OH, Z11-16:Ac, and Z9-16:Ald. Three subunits of the MGC (the CU, DA and DP) and one ordinary glomerulus (OG1) in the ALs were characterized. The CU is responsive to Z11-16:Ald and Z9-14:Ald, DA is to Z9-14:Ald and Z11-16:OH, DP is to Z11-16:Ac, and OG1 is to Z9-16:Ald. CU and DA are activated by mixtures of Z11-16:Ald and Z9-14:Ald, suggesting that the antagonistic information of Z9-14:Ald is integrated and processed in ALs or the higher center such as lateral horns (LHs). The antagonist signals in DA may suppress the pheromone signal in CU via AL local interneurons, or be directly conveyed to the LHs in a mostly stereotyped fashion, which finally changes behavioral outputs.

As MsepOR3 and MsepOR2 are expressed in different trichoid sensilla and their most effective ligands are Z11-16:Ald and Z9-14:Ald, respectively (Jiang et al., 2019 and this study), it would be reasonable to believe that the MsepOR3 neuron is located in the A type sensillum with its axon projects to the CU, while the MsepOR2 neuron is instead located in the B type sensillum with its axon projects to the DA in ALs. We speculate that the spikes of the A type sensillum induced by Z11-16:Ald and Z9-14:Ald were from the same OSN expressing MsepOR3 because: (1) the spikes induced by Z11-16:Ald and Z9-14:Ald in the A type sensillum had the same amplitude (Figs. 1 and 2); (2) MsepOR3 is tuned to Z11-16:Ald mainly, but also has a weak response to Z9-14:Ald (Jiang et al., 2019); (3) besides the DA, the CU was also responsive to Z9-14:Ald (Fig. 3); (4) MsepOR3 and MsepOR2 were expressed in OSNs of different sensilla (Fig. 8). We also speculate that three OSNs are located in each of B type sensilla: one OSN expressing MsepOR2 and projecting to DA, is responsive to Z9-14:Ald; the second OSN projecting to DP, is responsive to Z11-16:Ac; and the third OSN projecting to OG1, is responsive to Z9-16:Ald. A recent study on the ultrastructure of antennal sensilla in *M. separata* reported that one type of trichoid sensilla contains three dendrites (Chang et al., 2015), which provides the evidence for this speculation. However, it is still required to be validated further by single sensillum fills to stain individual neurons into the antennal lobe.

One very interesting result from our optical imaging is that Z9-16:Ald activated an ordinary glomerulus (OG1) in ALs of *M. separata* males. In general, OSNs tuned to different pheromone components target specific

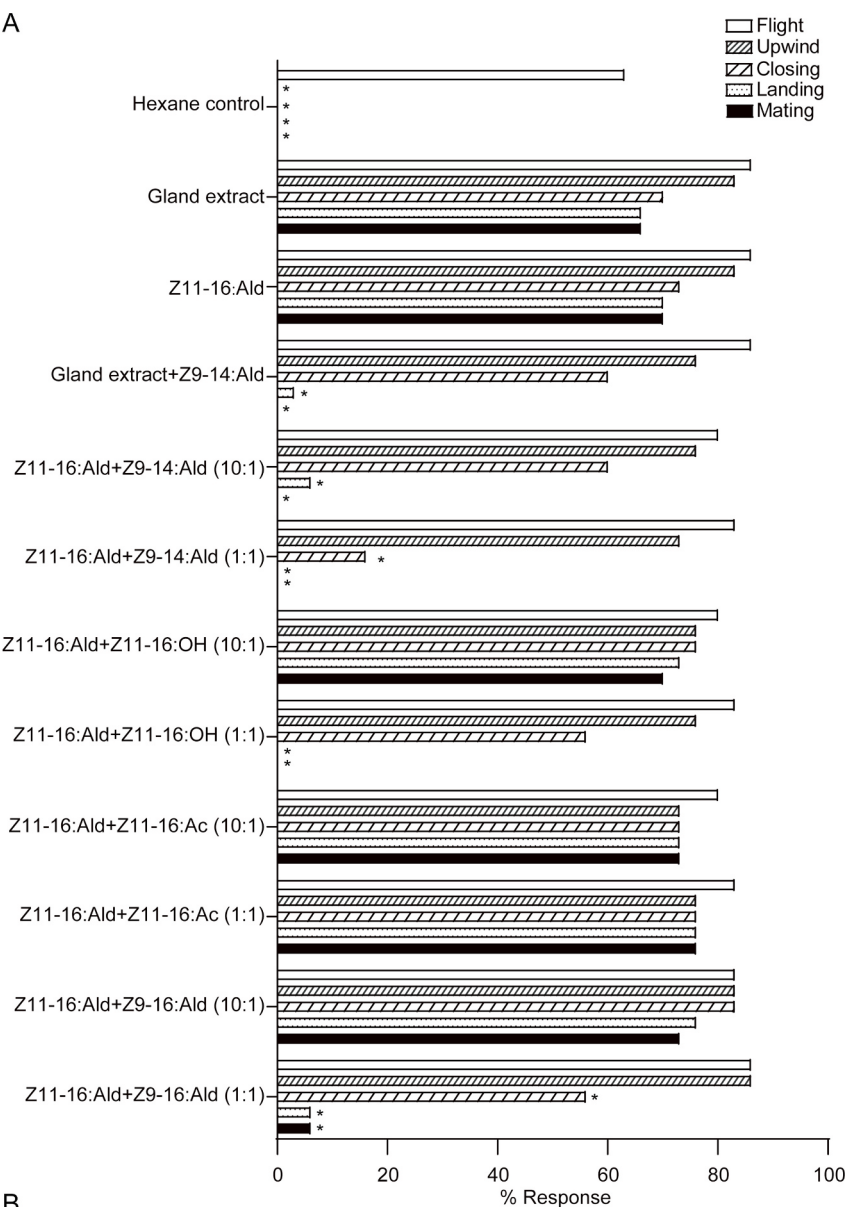
glomeruli of the MGC in moth species (Hansson et al., 1992). These enlarged glomeruli increase the sensitivity of moths toward sex pheromones (Hansson and Stensmyr, 2011). However, some exceptional cases suggest that some ordinary glomeruli in male ALs are also involved in detection of pheromonal compounds in some moth species. An early study by using single sensillum recording and neuron staining with cobalt discovered that one neuron housed in type II trichoid sensilla of *S. littoralis* male projects to an ordinary glomerulus (Ochieng et al., 1995). Further optical imaging and intracellular recording of projection neurons in *S. littoralis* found that the putative pheromone Z7-12:Ac is able to activate an ordinary glomerulus in the male of *S. littoralis* (Anton and Hansson, 1994, 1995; Carlsson et al., 2002). However, the receptors of these OG-activated pheromonal compounds are still needed to be identified in both *S. littoralis* and *M. separata*.

Another very interesting fact we find in this study is that the behavioral responses of *M. separata* males to pheromonal compounds in the wind tunnel is far more sensitive than the physiological responses in SSR and optical imaging. All behavior is the product of central nervous integration of overall stimuli from both outside and inside the insect (Kennedy, 1978). Since the insect antenna bears a large number of pheromone sensory neurons operating in parallel, the complex neural patterns cannot be assessed from only some sampled single sensillum recordings. Moreover, there could be other signal inputs from organs besides antennae. Most recently it is discovered that an OR expressed in the ovipositor also has a supplemental olfactory function in *H. assulta* (Li et al., 2020). In addition, the inner physiological state of insects can greatly modulate the sensitivity of sensilla and behavioral outputs. The limited resolution of optical imaging and SSR may also contribute to such a discrepancy.

### 3.2. The role of pheromone communication in reproductive isolation of sympatric noctuid species

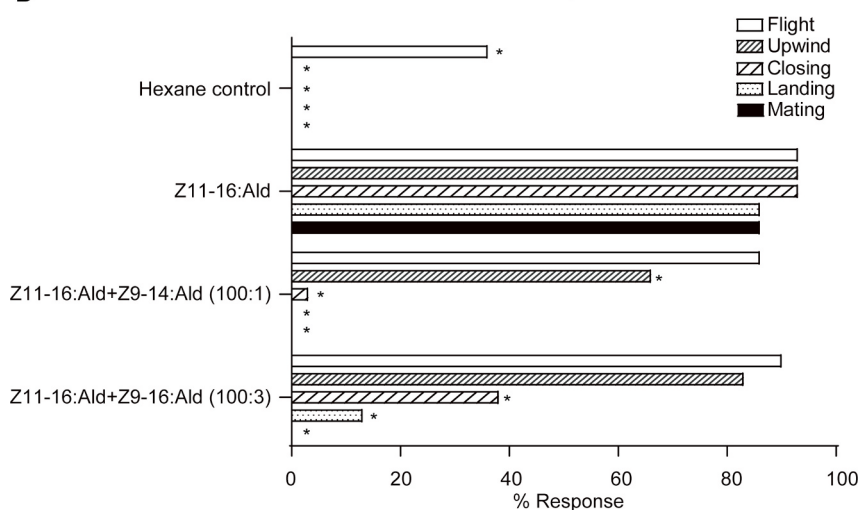
*M. separata* shares Z11-16:Ald as a pheromone component with almost all of *Helicoverpa* and *Heliothis* moth species, including *H. armigera*, *H. zea*, *H. punctigera*, *H. assulta*, *H. virescens*, and *H. subflexa* (Klun et al., 1980; Lee et al., 2006; Nesbitt et al., 1979; Roelofs et al.,

A



**Fig. 5. The behavioral responses of male *M. separata* to pheromone lures in the wind tunnel. (A)** The low dosage pheromone assay, using Z11-16:Ald at a dosage of 10 ng; **(B)** the high dosage pheromone assay, using Z11-16:Ald at a dosage of 1 µg. Hexane was used as a control. The star means that the percentage of the behavioral response is significantly different from that to the gland extract in the corresponding behavioral stage (Fisher's exact test,  $P < 0.05$ ,  $N = 30$  for each treatment).

B



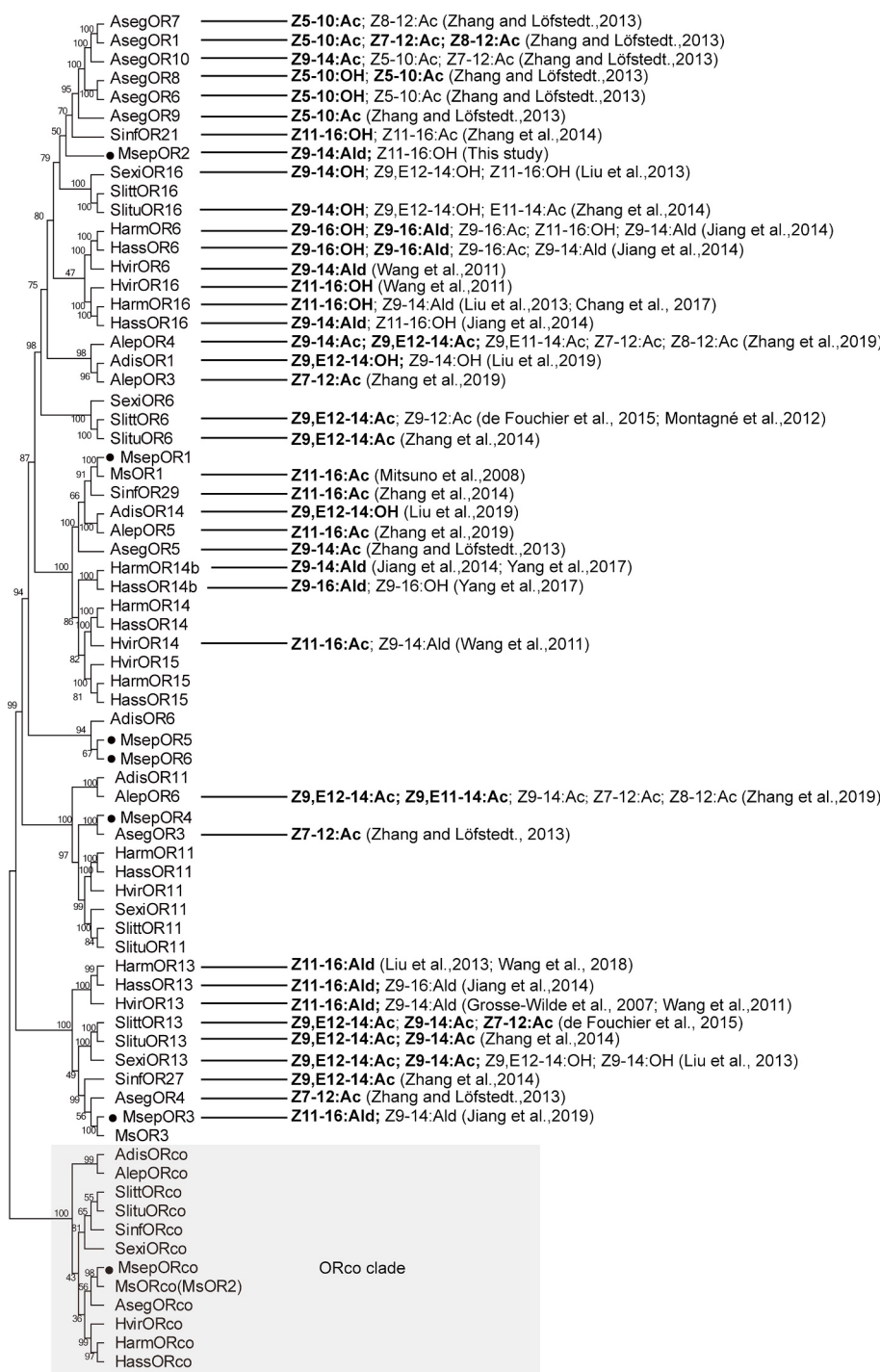


**Fig. 6. The phylogenetic tree and functional annotations of pheromone receptors in noctuid species.** Bootstrap values are based on 1000 replicates. Harm, *Helicoverpa armigera*; Hass, *Helicoverpa assulta*; Msep, *Mythimna separata* in this study (indicated by a black circle); Ms, *M. separata* from reported from a Japanese population (Mitsuno et al., 2008); Hvir, *Heliothis virescens*; Sinf, *Sesamia inferens*; Aseg, *Agrotis segetum*; Alep, *Athetis lepigone*; Slit, *Spodoptera littoralis*; Slitu, *Spodoptera litura*; Sexi, *Spodoptera exigua*; Adis, *Athetis dissimilis*. For functionally characterized receptors, their most effective ligands are bolded.

1974; Rothschild et al., 1982; Teal et al., 1981; Wang et al., 2005). In the terms of pheromone communication, how *M. separata* keeps behavioral isolation from this group of species is an intriguing question. Among *Heliothis/Helicoverpa* species, *H. armigera* is the only sympatric noctuid species of *M. separata* using Z11-16:Ald as a major pheromone component in North China, and both of them are major pests in the corn field. The sex pheromone blend of *H. armigera* contains Z11-16:Ald and Z9-16:Ald at the ratio of about 100:3 (Cork et al., 1992; Kehat et al., 1980; Nesbitt et al., 1980; Wang et al., 2005). Addition of Z9-16:Ald to the lure containing 1 µg Z11-16:Ald at the ratio of 3:100 significantly inhibited the upwind and closing behaviors of *M. separata* males (Fig. 5B). Besides Z9-16:Ald, about 0.25–1.5% Z9-14:Ald was present in the female pheromone gland of *H. armigera*, and 0.3% Z9-14:Ald in combination

with the binary pheromone blend trapped more *H. armigera* males in the field (Zhang et al., 2012). Z9-14:Ald is also a pheromone component of *H. virescens* with the ratio of 1:16 to Z11-16:Ald (Tumlinson et al., 1975; Klun et al., 1989). The wind tunnel assays show that addition of Z9-14:Ald with three ratios (1:1, 1:10, and 1:100) all strongly inhibited the attractiveness of Z11-16:Ald to *M. separata* males (Fig. 5). Clearly, the presence of Z9-16:Ald and Z9-14:Ald in the pheromone glands plays an important role in intraspecific and interspecific chemical communications of *H. armigera*.

In *H. armigera*, the pheromone detection system is even more complicated (Fig. 9). Three types of sensilla are involved in olfactory coding for its sex pheromone. The A type sensilla respond to Z11-16:Ald, the B type sensilla respond to Z9-14:Ald, and the C type sensilla respond

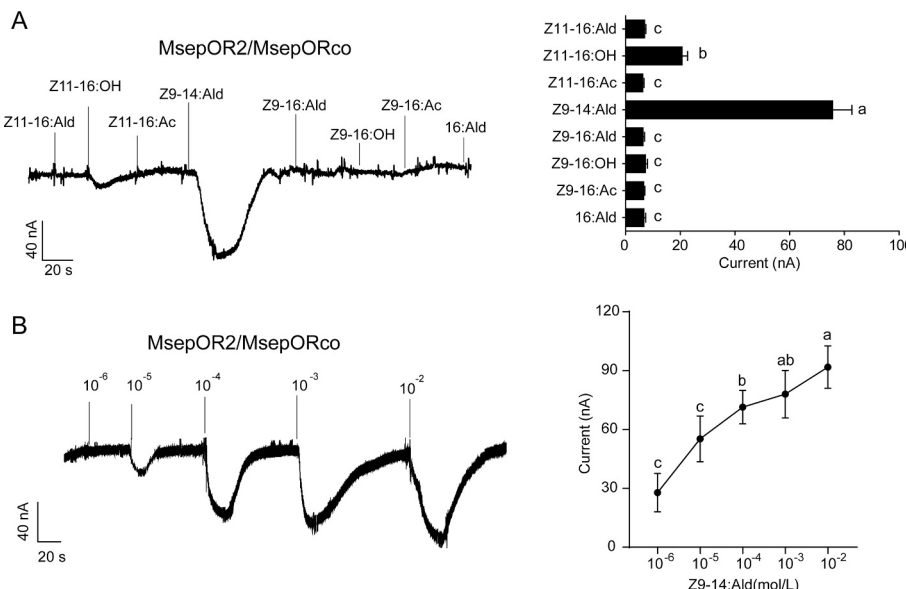


**Fig. 7. Responses of *Xenopus* oocytes co-expressing MsepOR2/MsepORco to intra- and interspecific pheromonal compounds. (A)** Responses to the compounds at  $10^{-4}$  M. Left: Inward current responses of the oocytes. Right: Response profiles of the oocytes (N = 22). **(B)** The concentration-responses of the oocytes to Z9-14:Ald. Left: Inward current responses of the oocytes. Right: the concentration-response curve (N = 5). The data in the right are presented as mean  $\pm$  SE, and the values with different letters are significantly different (ANOVA & Tukey HSD multiple comparison,  $P < 0.05$ ).

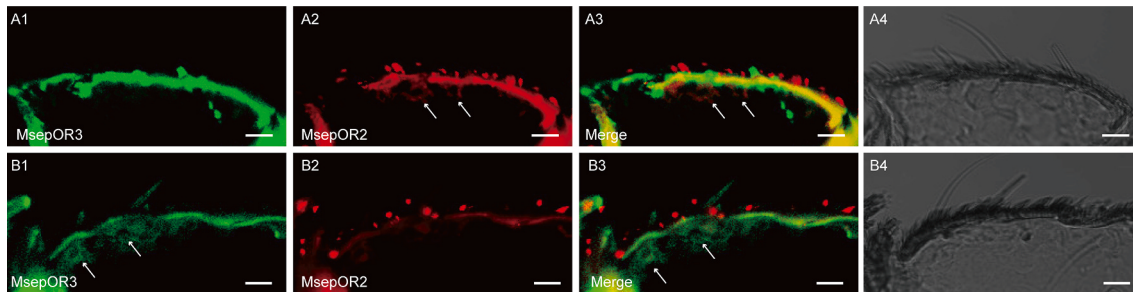
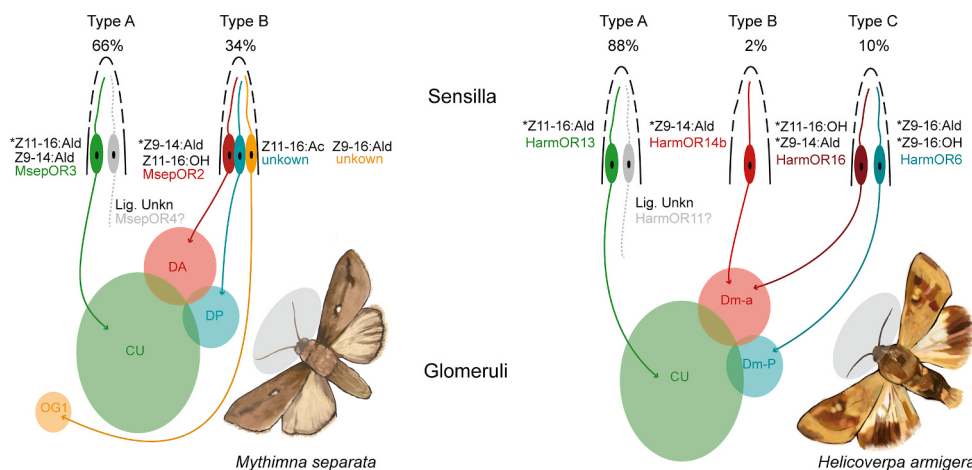


**Fig. 8. The localization of MsepOR3 and MsepOR2 in antennae of male *M. separata* by double fluorescence *in situ* hybridization.** Biotin-labeled probes antisense RNA probes for MsepOR3 transcripts (A1 and B1, green). Digoxin-labeled probes antisense RNA probes for MsepOR2 transcripts (A2 and B2, red). Merge red and green fluorescence of MsepOR3 and MsepOR2 transcripts (A3 and B3). Bright-field images are presented as references (A4 and B4). Arrows indicate the cell location. Scale bars: 10  $\mu$ m.



to Z9-16:Ald, Z9-14:Ald, Z11-16:OH, and Z11-16:Ac (Chang et al., 2016; Wu et al., 2013, 2015; Xu et al., 2016, 2017). It is speculated that in the A type sensillum, one OSN expressing HarmOR13 is tuned to Z11-16:Ald specifically; in the B type sensillum, one OSN expressing HarmOR14b is tuned to Z9-14:Ald; and in the C type sensillum, one OSN expressing one PR is tuned to Z9-16:Ald (possibly HarmOR6 but its most effective ligand

is (Z)-9-hexadecenol), and another OSN expressing HarmOR16 is tuned to Z11-16:OH (Chang et al., 2017; Jiang et al., 2014; Liu et al., 2013; Yang et al., 2017; Zhang et al., 2010). In the ALs, three subunits of the MGC (the CU, Dm-P and Dm-A) are responsive to the pheromone and related compounds: the CU is responsive to Z11-16:Ald only, Dm-P is to Z9-16:Ald and Z9-14:Ald, and Dm-A is to Z9-14:Ald, Z11-16:OH,

Z11-16:Ac, which are all behavioral antagonists of *H. armigera* (Wu et al., 2013, 2015; Xu et al., 2016).

Comparing the pheromone detection systems of the two species, we can find the pheromone sensilla have differences in functional types and their responding profiles, but the structural frame and elements at peripheral and central levels are quite similar. The orthologous PRs between *M. separata* and *H. armigera* have similarity in the sequence, and their functions seem also conservative. MsepOR3 shares 63% identity with HarmOR13 in the amino acid sequence, and both of them are primarily tuned to Z11-16:Ald (Jiang et al., 2019; Liu et al., 2013; Zhang et al., 2010); MsepOR2 shares 55% identity with HarmOR14b, and both of them are specifically tuned to Z9-14:Ald (Jiang et al., 2014, 2019). Moreover, *M. separata* also shares characteristics in the olfactory pathways for pheromonal components and antagonists with *H. armigera*. In the two species, the OSNs sensing the essential or major pheromone component are the most abundant in the male antennae, and their axons always project to the CU of MGC in ALs. Moreover, both systems have the OSNs to detect the behavioral antagonist, particularly Z9-14:Ald and project to one subunit of MGC. Such similarities in the pheromone communication channel of the two species may give rise to some attractions of both species by the Z11-16:Ald-based synthetic sex attractants in the field. However, the different coding mechanisms for Z9-16:Ald, Z9-14:Ald and Z11-16:Ac in two species may mainly contribute to behavioral isolation between *M. separata* and *H. armigera*. Other possible differences in times of mating, male pheromones, and phenology and habitat between the two species could promote their reproductive isolation.

### 3.3. Evolution of Z9-14:Ald as a pheromone antagonist in *M. separata*

The field experiments with many moth species showed that addition of very small amounts of pheromone components from a closely related species can abolish the attractiveness of a pheromone, and males of these species have olfactory pathways that are specifically attuned to these antagonists (Cardé and Haynes, 2004; Carlsson et al., 2002; Löfstedt et al., 1991; Vickers et al., 1998). It is clear that communication interference is the principal selective force for evolution of such specialized pathways and behavioral avoidance of their own pheromone tainted with antagonists (Löfstedt, 1993). Likewise, Z9-14:Ald acting as a pheromone antagonist of *M. separata* is not presented in the female pheromone gland extracts, while the OSNs responding this compound are abundant in the male antennae. Why Z9-14:Ald was selected by males as an important coding target? We consider there are two possible reasons. Firstly, in the terms of chemical structure, Z9-14:Ald is a close analog mimicking Z11-16:Ald. Although their straight chain molecules have 2 carbon difference in length, the two compounds share an aldehyde group in one end and a double bond with Z configuration in the same position from the other end (Fig. 10). With such a structural similarity, it is not surprising that MsepOR3 mainly tuned to Z11-16:Ald also has a weak response to Z9-14:Ald (Jiang et al., 2019), and the OSNs in the A type sensilla and the CU in ALs are responsive to the two compounds in *M. separata*. Obviously, if just based on the MsepOR3-CU pathway in the male olfactory system, *M. separata* would be risky in finding the right partner because the males could not distinguish Z9-14:

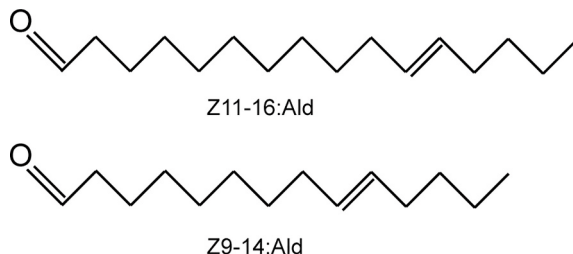


Fig. 10. The chemical structures of Z11-16:Ald and Z9-14:Ald.

Ald from Z11-16:Ald. The MsepOR2-DA pathway specifically coding for Z9-14:Ald as a behavioral antagonist makes up for this deficiency. Secondly, in the terms of chemical ecology, Z9-14:Ald is a significant element in shaping pheromone communication systems of moth species. It is widely used as a semiochemical in moth species, especially *Heliothis* and *Helicoverpa* species. In *Heliothis virescens* (Klun et al., 1980; Roelof et al., 1974; Tumlinson et al., 1975) and *Heliothis peltigera* (Dunkelblum and Kehat, 1989), Z9-14:Ald is a principal pheromone component, while in their closely related species *Helicoverpa zea*, *Helicoverpa armigera* and *Helicoverpa assulta* (Shaver et al., 1982; Vickers et al., 1991; Wu et al., 2015), it is conversely used as a pheromone antagonist and decreases male attraction. The sensilla responding to Z9-14:Ald are abundant on the male antennae of all these species. In this study, we disclose that *M. separata* has a similar pathway for this antagonist as these species. From this point of view, *M. separata* could be closely related with *Heliothis* and *Helicoverpa* species in the phylogeny of noctuid moths.

In summary, for the males of *M. separata* to detect the sex pheromone, one primary olfactory pathway coding for Z11-16:Ald is not enough because it also responds to a structurally similar compound, Z9-14:Ald. To close that loophole, the insects use another pathway to recognize Z9-14:Ald as a behavioral antagonist. We propose that it is the OSNs expressing MsepOR2 in the B type sensilla respond to Z9-14:Ald, and then project to the DA of MGC, and finally mediate such an antagonistic effect. The high similarity of PR functions and related olfactory pathways of *M. separata* with *Heliothis* and *Helicoverpa* species indicate that general patterns of pheromone and pheromone antagonist reception and processing are conserved within noctuid moth species.

## 4. Methods and materials

### 4.1. Insects

The Oriental armyworm larvae were reared on an artificial diet in the laboratory at  $25 \pm 1$  °C (Jiang et al., 2019). After pupating, pupae were distinguished by sex. Adults were fed 10% honey water after emergence and at a photoperiod of 16:8 h light: dark.

### 4.2. Pheromone chemicals

The pheromonal compounds used in this study are listed in Table 1. GC-MS (6890N GC and 5973 MS) was used for analysis and identification of impurities in lower-purity pheromonal compounds. The purity of Z9-14:Ald is 93.7%, and the impurities are consisted of 3-trifluoroacetoxypentadecane, butyl hexanoate, and hexadecamethylheptasiloxane at 1.5%, 3.3%, 1.5%, respectively.

### 4.3. Single sensillum recording (SSR) preparation and testing

SSR was used to identify responses to sex pheromones of the long trichoid sensilla in male antennae. All pheromonal compounds were dissolved in the paraffin oil, and the paraffin oil was used as the control. When we tested sensilla response profiles, the pheromonal compounds were loaded 100 µg (loading 10 µL of the 10 µg/µL solution). In dose-

Table 1

The pheromonal compounds of *Mythimna separata* and *Helicoverpa armigera* used in the experiments.

Pheromone compounds	Purity (%)	Company	CAS number
Z9-16:Ald	>90	Shin-Etsu	56219-04-06
Z11-16:Ald	>92	Shin-Etsu	53939-28-9
16:Ald	>92	Shin-Etsu	629-80-1
Z9-14:Ald	>93	Shin-Etsu	53939-27-8
Z9-16:OH	>98	Sigma-Aldrich	10378015
Z11-16:OH	>92	Shin-Etsu	56683-54-6
Z9-16:Ac	>90	Shin-Etsu	34010-20-3
Z11-16:Ac	>92	Shin-Etsu	34010-21-4

response experiments, the contents of the tested pheromonal compounds (Z11-16:Ald, Z9-14:Ald, Z11-16:Ac, Z11-16:OH, Z9-16:Ald) were used 1 µg, 10 µg, 100 µg and 1000 µg. When we compared the responses of A type sensilla to Z11-16:Ald, Z9-14:Ald and their mixtures, the dosages of 50 µg and 100 µg were used for each compound, and 50 + 50 µg and 100 + 100 µg were used for their mixtures.

The fixing and recording methods conducted following the methods described by Xu et al. (2016). Each male moth was placed into a 1 mL pipette and immobilized by dental wax. Sensilla tips were cut off with sharpened forceps. Reference electrodes were inserted into a compound eye, and an Ag–AgCl electrode was placed in another glass micropipette that was filled with lymph saline to record action potentials. A steel tube (diameter, 6 mm; length, 15 cm) was positioned 2 cm from the antenna. The purified and humidified air passed over the antenna (12.5 mL/s). Test odors were added to filter paper (1 cm × 0.5 cm) which placed into a Pasteur pipette. The air stream came from a stimulus flow controller CS-55 (Syntech, Buchenbach, Germany), which generated 200 ms air pulses through the odor cartridge at a flow rate of 10 mL/s, and a compensating air flow was provided to maintain a constant current. To avoid the sensory adaptation during recordings, each stimulus of pheromone compounds was presented at random with an interval of at least 20 s. In dose-response experiments, the antenna was stimulated with a given compound from low to high doses. The recorded signals were then amplified through an IDAC interface amplifier IDAC-4 (Syntech, Buchenbach, Germany). Autospike 3.4 (Syntech, Buchenbach, Germany) was used to store and analyze data. Action potential frequencies (spikes/s) were calculated by counting the number of spikes that occurred during 1 s of the response.

#### 4.4. In vivo optical imaging methods of male ALs to pheromonal compounds

To investigate the neural representations of pheromonal compounds in male antennal lobes (AL), we tested the electrophysiological active compounds based on SSR results: Z11-16:Ald, Z11-16:OH, Z11-16:Ac, Z9-16:Ald, and Z9-14:Ald. Each pheromonal compound was dissolved in paraffin oil, and loaded 100 µg. Paraffin oil was used as the control. To studied the spatial relationships of glomeruli which activated by Z11-16:Ald and Z9-14:Ald, we set three mixtures (named as Mix 1, Mix 2, Mix 3) of these two pheromonal compounds: Mix 1, the mixture of Z11-16:Ald 100 µg and Z9-14:Ald 1 µg; Mix 2, the mixture of Z11-16:Ald 100 µg and Z9-14:Ald 10 µg; and Mix 3, the mixture of Z11-16:Ald 100 µg and Z9-14:Ald 100 µg. In dose-response experiments, the serial dosages (1 µg, 10 µg, 100 µg and 1000 µg) of Z11-16:Ald and Z9-14:Ald were used.

The *in vivo* optical imaging methods were conducted as previously described (Bisch-Knaden et al., 2018; Galizia et al., 2000; Jiang et al., 2019; Wu et al., 2013, 2015). Put the male moth into an opened plastic tube and fixed this tube in a custom-made chamber. Fixed moths with dental wax. Then removed all the head scales, muscles and mouthparts tissues and made a window between the two compound eyes. Kept the brain (including antennal lobes) in Ringer solution. CaGR-2-AM (Molecular Probes, Eugene, OR, USA) was used as the staining material. Before staining, mixed the CaGR-2-AM with Pluronic-127 and then diluted in Ringer solution. When staining, dropped the diluted dye into moth head and placed moths in the dark for 1 h at 12 °C. After staining, the brain was rinsed several times with Ringer solution and ready for imaging. Each stimulus solution was first added into a filter paper (1 cm × 0.5 cm) in Paster pipette and then the Paster pipette was connected into the air stream using a stimulus flow controller CS-55 (Syntech, Buchenbach, Germany), which generated 200 ms air pulses through the odor cartridge at a flow rate of 10 mL/s. Each stimulus of pheromone compounds was presented at random with an interval of at least 20 s. In dose-response experiments, the antenna was stimulated with a given compound from low to high doses.

When observed, an upright microscope Olympus BX51WI (Olympus, Tokyo, Japan) with a 20 × Olympus NA 0.95 water immersion objective

(Olympus, Tokyo, Japan) was used. We used Till Photonics imaging system (Till Photonics, Gräfelfing, Germany) to collect data. For each stimulus, the stimulation occurs at the frame 12 among totally 40 continuous frames. The background defined as the mean fluorescence (F) of frames 2–11. For each frame, the ratio of the frame against the background ( $F_n/F$ ,  $n = 1–40$ ) was calculated. After smoothed (to reduce the noise), the value of  $F_n/F$  defined as  $F_n/F$  (smooth, 30 frames). The fluorescence change value ( $\Delta F/F$ ) was define as  $\Delta F/F = F_n/F - F_n/F$  (smooth, 30 frames). The smooth treatment can reduce noise but not remove pertinent signals. We then used the ROI (region of interesting) method (Tang et al., 2020) to capture the  $\Delta F/F$  value of active region from all 40 frame through ImageJ software (NIH, Bethesda, MA, USA). The mean of three sequential frames at the signal's maximum was taken as the amplitude of odor-induced responses. The average of the responses elicited by each stimulus was calculated from all tested replicates. Based on the AL atlas of male *M. separata* (Jiang et al., 2019), we were able to identify the activated MGC subunits according to their position and outline. When we overlapped the pseudo-color graph with the grey graph, the color threshold was adjusted to get the highest signal/noise graph by using ImageJ software (NIH, Bethesda, MA, USA). To avoid cutting off signals, we compared signal positons and repeatability in all the replicates. Pheromone stimulation patterns showed in the overlapped graph were come from the same tested moth.

#### 4.5. Preparation of pheromone gland extracts

For the wind tunnel test, the sex pheromone gland extracts were prepared and obtained from the calling females of 4-day-old. When female calling behavior occurred, the abdominal tip (including the sex pheromone gland) was excised with a micro-scissor. A total of 50 tips were immersed in 500 µL hexane solvent (10 µL per female) for 20 min at ambient temperature. After removing the pheromone gland, samples were stored at –20 °C.

For gas chromatography coupled with mass spectrometry (GC-MS), the extracts of individual pheromone glands were prepared. Each tip was immersed in 6 µL hexane for 20 min at ambient temperature, then the tip was removed, and the extract was stored at –20 °C. We collected female tips in the scotophase from 1-day-old to 7-day-old of female moths. To obtain the tips of mated females, we put 10 females (3-day-old) together with 12 males in the same cage. After two nights, we excised the tips of females and immersed each tip in 6 µL hexane for 20 min at ambient temperature.

#### 4.6. GC-MS analysis of the pheromone gland extracts

Pheromone gland extracts were further analyzed by GC-MS. Agilent Technologies 5973 MS (Agilent Technologies, Santa Clara, CA, USA) coupled with an Agilent Technologies 6890N GC (Agilent Technologies, Santa Clara, CA, USA) equipped with an HP-5 capillary column (30 m × 0.25 mm ID, 0.25 µm film; J&W Scientific, Folsom, CA, USA) were used. Injector temperature was 220 °C, and the GC oven temperature was programmed to 60 °C for 1 min, then increased to 250 °C at a rate of 10 °C per min. The detector temperature was 250 °C. Injection was performed in splitless mode and helium was used as the carrier gas. Windows NT/MASS Spectral Search Program 1.7 (Agilent Technologies, Santa Clara, CA, USA) was used for data analysis. Voltage for electron impact ionization in mass spectra was 70 eV. The temperatures of the ion source and the interface were 230 °C and 280 °C, respectively.

#### 4.7. The wind tunnel bioassays

The behavioral bioassays were performed in a wind tunnel. Pheromonal compounds were dissolved in hexane. One piece of filter paper (2 cm × 1 cm) loading with 10 µL of a given pheromone solution was used as a lure. The low and high doses of pheromones were used in the bioassays. In the low dose pheromone assay, 12 lures with different

components or ratios were used: (1) Hexane as the control; (2) the pheromone gland extracts with 1 FE (female equivalent); (3) 10 ng Z11-16:Ald; (4) the pheromone gland extracts with 1 FE + 1 ng Z9-14:Ald; (5) 10 ng Z11-16:Ald + 1 ng Z9-14:Ald; (6) 10 ng Z11-16:Ald + 10 ng Z9-14:Ald; (7) 10 ng Z11-16:Ald + 1 ng Z11-16:OH; (8) 10 ng Z11-16:Ald + 10 ng Z11-16:OH; (9) 10 ng Z11-16:Ald + 1 ng Z11-16:Ac; (10) 10 ng Z11-16:Ald + 10 ng Z11-16:Ac; (11) 10 ng Z11-16:Ald + 1 ng Z9-16:Ald; (12) 10 ng Z11-16:Ald + 10 ng Z9-16:Ald. In the high dose pheromone assay, 4 lures with different components or ratios were used: (1) Hexane as the control; (2) 1 µg Z11-16:Ald; (3) 1 µg Z11-16:Ald + 30 ng Z9-16:Ald; (4) 1 µg Z11-16:Ald + 10 ng Z9-14:Ald.

The wind tunnel had a size of 2.5 m × 1 m × 1 m (L × W × H), and the wind speed was about 0.5 m/s. The environmental condition was 22°C–25 °C, 20%–40% humidity, and 0.5 lux of diffusive red light from the top. Every male moth was released and tested for 5 min. The new lure was used for each moth which was tested only for one time. Male behavioral responses were recorded in the following five typical categories: (1) flight: male moths took off from the release cage; (2) upwind: male moths showed a characteristic zigzag pursuing flight pattern toward the pheromone source and reached ≤ 70 cm from the lure; (3) closing: male moths reached 10 cm from the pheromone source; (4) landing: male moths landed on the lure; (5) mating: male moths climbed the lure and extruded the hair-pencils from the abdominal cavity. Thirty males were tested for each treatment in the two experiments.

#### 4.8. Pheromone receptors conservation and phylogenetic analyses

We sequenced the antenna transcriptome of both males and females and identified 6 putative pheromone receptors (Jiang et al., 2019). Although recently several studies on transcriptome analyses of *M. separata* antennae or heads were carried out (Bian et al., 2017; Chang et al., 2017; Du et al., 2017; He et al., 2017; Liu et al., 2017), most of the sequences of putative PRs have not been revealed to the public. The related genes of other Noctuidae moth species, *Sesamia inferens*, *Agrotis segetum*, *H. virescens*, *H. armigera*, *H. assulta*, *S. littoralis*, *Spodoptera litura*, *Athetis lepigone*, *Athetis dissimilis* and *M. separata* (Japanese population), were download from NCBI. ORcos were used as outgroups. All phylogenetic trees were constructed using the neighbor-joining method implemented in MEGA6 (Tamura et al., 2013) with default settings and 1000 bootstrap replicates. We also summarized the ligands of pheromone receptors previously reported in the phylogenetic trees (Chang et al., 2017; de Fouchier et al., 2017; Jiang et al., 2014, 2019; Liu et al., 2013, 2019; Mitsuno et al., 2008; Montagné et al., 2012; Wang et al., 2010; Zhang et al., 2014; Yang et al., 2017; Zhang et al., 2014, 2014, 2019; Zhang and Löfstedt, 2013). We used PRALINE multiple sequence alignment (<http://www.ibi.vu.nl/programs/pralinewww/>) for the conservation analysis (Simossis and Heringa, 2003, 2005).

#### 4.9. Functional analysis of the pheromone receptor *MsepOR2*

Total RNA was isolated from the antennae with TRIzol reagent (Invitrogen, Carlsbad, CA, USA) and then cDNA was synthesized with M-MLV Reverse Transcriptase (Promega, Madison, WI, USA). The primer sequences of *MsepOR2* and *MsepORco* are listed in Table S1. The PCR program was 98 °C for 30 s; 98 °C for 10 s, 52 °C for 30 s, and 72 °C for 30 s for 35 cycles; and 72 °C for 2 min. The coding sequences of *MsepOR3* and *MsepORco* were cloned into pGEM-T easy vector (Promega, Madison, WI, USA), and then cloned into pCS2+ vector. The pCS2+ vectors were linearized using NotI (Takara Shuzo, Shiga, Japan), and cRNAs were synthesized from the linearized pCS2+ vectors with mMACHINE SP6 (Ambion, Austin, TX, USA). cRNAs were dissolved in RNase-free water and stored at -80 °C.

Two-electrode voltage clamp recording was used to detect the whole cell current. All tested pheromonal compounds were at the concentration of 10<sup>-4</sup> M. In the dose-response test, serial compound concentrations from 10<sup>-6</sup> M, 10<sup>-5</sup> M, 10<sup>-4</sup> M, 10<sup>-3</sup> M, to 10<sup>-2</sup> M were used.

Mature and healthy oocytes were microinjected with 23 nL (50 ng) of *MsepOR2* and *MsepORco* cRNA mixtures at a 1:1 ratio. Oocytes injected with water were used as a negative control. Injected oocytes were incubated for 3–4 d at 16 °C in a bath solution (96 mM NaCl, 2 mM KCl, 1 mM MgCl<sub>2</sub>, 1.8 mM CaCl<sub>2</sub>, and 5 mM HEPES, pH 7.5) supplemented with 100 mg/mL gentamycin and 550 mg/mL sodium pyruvate.

The recording method was the same as described by Jiang et al. (2019). Whole cell currents were recorded with a two-electrode voltage clamp. Intracellular glass electrodes were filled with 3 M KCl and had resistances of 0.2–2.0 MΩ. Signals were amplified with an OC-725C amplifier (Warner Instruments, Hamden, CT, USA) at a holding potential of -80 mV, low-pass filtered at 50 Hz, and digitized at 1 kHz. Data acquisition and analysis were carried out with Digidata 1322A and pCLAMP (Axon Instruments, Foster, CA, USA).

#### 4.10. In situ hybridization

Two-color double *in situ* hybridizations were performed following protocols reported previously (Krieger et al., 2004; Yang et al., 2017). The primers of *MsepOR3* and *MsepOR2* probes were listed in Table S2. Both digoxin (Dig)-labeled and biotin (Bio)-labeled probes were synthesized by DIG RNA labeling Kit version 12 (SP6/T7) (Roche, Mannheim, Germany). Antennae were dissected from 4 day old male moths, embedded in JUNG tissue freezing medium (Leica, Nussloch, Germany). Sections (12 µm) were prepared with a Leica CM1950 microtome at -22 °C, then mounted on SuperFrost Plus slides (Thermo Scientific, Waltham, MA, USA). 100 µL hybridization solution (Boster, Wuhan, China) containing both Dig and Bio probes was placed onto the tissue sections. After hybridization, slides were washed in saline sodium citrate (SSC), treated with 1% blocking reagent (Roche, Mannheim, Germany), and then incubated with anti-digoxigen (Roche, Mannheim, Germany) and Streptavidin-HRP (PerkinElmer, Boston, MA, USA). The sections were incubated with HNPP/Fast Red (Roche, Mannheim, Germany) and then with Biotinyl Tyramide Working Solution followed by the tyramide signal amplification kit protocols (PerkinElmer, Boston, MA, USA) and finally mounted in Anti-Fade Mounting Medium (Beyotime, Beijing, China). All the sections were analyzed under a Zeiss LSM710 Meta laser scanning microscope (Zeiss, Oberkochen, Germany).

#### 4.11. Statistics and data analysis

Statistical analysis was carried out using SPSS 16.0 (IBM, Chicago, IL, USA) if not otherwise specified. The SSR were analyzed with Auto-spike V3.9 (Syntech, Buchenbach, Germany). Wind tunnel test data were analyzed using GraphPad Prism 5 (GraphPad Software, La Jolla, CA, USA). The *in vivo* optical imaging data acquired with Till-vision (Till Photonics, Gräfelfing, Germany) were analyzed by ImageJ 1.43m (NIH, Bethesda, MA, USA) and custom-made programs in MATLAB R2009a (The Math Works, Natick, MA, USA). For the *Xenopus* oocyte expression system and two-electrode voltage-clamp recording, data acquisition and analysis were carried out with Digidata 1322A and pCLAMP (Axon Instruments, Foster, CA, USA). Dose response data were analyzed using GraphPad Prism 5 (GraphPad Software, La Jolla, CA, USA). All the statistical details are provided in the supplementary 1.

#### Ethics

**Animal experimentation:** All procedures in this study were approved by the Animal Care and Use Committee of the Institute of Zoology, Chinese Academy of Sciences for the care and use of laboratory animals (protocol number IOZ17090-A). The *Xenopus laevis* was anesthetized 30 min by bath in the ice and the wounds were carefully treated to avoid infection. Every effort was made to minimize suffering.

## Acknowledgement

We thank our colleagues Meng Xu and Ke Yang for their assistances in single sensillum recording and *in situ* hybridization; Bill Hansson and Markus Knaden from Max Planck Institute for Chemical Ecology for their

comments to the manuscript. This work was supported by the Key Research Program of the Chinese Academy of Sciences (Grant No. KJZD-SW-L07) and the National Natural Science Foundation of China (Grant No. 31830088, 31772528).

## Appendix A. Supplementary data

Supplementary data to this article can be found online at <https://doi.org/10.1016/j.ibmb.2020.103439>.

## Appendix B

Table S1 The primers for cloning the full length cDNA sequences of *MsepOR2* and *MsepORco*.

Gene	Enzyme cutting site	Primer sequences (5'-3')
<i>MsepORco</i>	EcoRI/F	<u>GAATTGCCACCATGATGACCAAAGTGAAGGC</u>
	XhoI/R	<u>CTCGAGTTACTTGAGTTGACCAAC</u>
<i>MsepOR2</i>	EcoRI/F	<u>GAATTGCCACCATGACTTAAGATCATTCTGTTGAAAT</u>
	XhoI/R	<u>CTCGAGTCACACGCTACGTAGAAAAGTGAAGTAAGA</u>

Note: F: forward strand; R: reverse strand; the underlined indicate restriction recognition sites, the bold indicate Kozak sequence.

Table S2  
The primers of *MsepOR3*, *MsepOR2* for *in situ* hybridization.

Gene	F/R	Primer sequences (5'-3')
<i>MsepOR2</i>	F	TAAAGGGCATTAACACACCATCTGATTA
	R	TCCTCTTGGAAATATTCTCAGCTCTTA
<i>MsepOR3</i>	F	TATTTCTGAATGAAATGCACCTTTTA
	R	CTATCCCTGGTCTCCATGTACTCCAAAG

Note: F: forward strand; R: reverse strand.

## References

- Allison, J.D., Cardé, R.T., 2016. Pheromones: reproductive isolation and evolution in moths. In: Allison, J.D., Cardé, R.T. (Eds.), Pheromone Communication in Moths: Evolution, Behavior, and Application. University of California Press, Oakland, California, pp. 11–23.
- Anton, S., Hansson, B.S., 1994. Central processing of sex pheromone, host odour, and oviposition deterrent information by interneurons in the antennal lobe of female *Spodoptera littoralis* (Lepidoptera: Noctuidae). *J. Comp. Neurol.* 350, 199–214.
- Anton, S., Hansson, B.S., 1995. Sex pheromone and plant-associated odour processing in antennal lobe interneurons of male *Spodoptera littoralis* (Lepidoptera: Noctuidae). *J. Comp. Physiol.* 176, 773–789.
- Baker, T.C., 2008. Balanced olfactory antagonism as a concept for understanding evolutionary shifts in moth sex pheromone blends. *J. Chem. Ecol.* 34, 971–981.
- Baker, T.C., Fadamiro, H.Y., Cosse, A.A., 1998. Moth uses fine tuning for odour resolution. *Nature* 393, 530–530.
- Baker, T.C., Ochieng, S.A., Cosse, A.A., Lee, S.G., Todd, J.L., Quero, C., Vickers, N.J., 2004. A comparison of responses from olfactory receptor neurons of *Heliothis virescens* to components of their sex pheromone. *J. Comp. Physiol.* 190, 155–165.
- Berg, B.G., Almaas, T.J., Bjaalie, J.G., Mustaparta, H., 1998. The macroglomerular complex of the antennal lobe in the tobacco budworm moth *Heliothis virescens*: specified subdivision in four compartments according to information about biologically significant compounds. *J. Comp. Physiol.* 183, 669–682.
- Berg, B.G., Almaas, T.J., Bjaalie, J.G., Mustaparta, H., 2005. Projections of male-specific receptor neurons in the antennal lobe of the Oriental tobacco budworm moth, *Helicoverpa assulta*: a unique glomerular organization among related species. *J. Comp. Neurol.* 486, 209–220.
- Berg, B.G., Tumlinson, J.H., Mustaparta, H., 1995. Chemical communication in heliothine moths IV. Receptor neuron responses to pheromone compounds and formate analogues in the male tobacco budworm moth *Heliothis virescens*. *J. Comp. Physiol.* 177, 527–534.
- Bian, H.X., Ma, H.F., Zheng, X.X., Peng, M.H., Li, Y.P., Su, J.F., Wang, H., Li, Q., Xia, R.X., Liu, Y.Q., Jiang, X.F., 2017. Characterization of the adult head transcriptome and identification of migration and olfaction genes in the oriental armyworm *Mythimna separata*. *Sci. Rep.* 7, 2324.
- Bierl, B.A., Beroza, M., Collier, C.W., 1970. Potent sex attractant of the gypsy moth: its isolation, identification, and synthesis. *Science* 170, 87–89.
- Bisch-Knaden, S., Dahake, A., Sachse, S., Knaden, M., Hansson, B.S., 2018. Spatial representation of feeding and oviposition odors in the brain of a hawkmoth. *Cell Rep.* 22, 2482–2492.
- Butenandt, A., Hecker, E., Hopp, M., Koch, W., 1962. Über den sexuallockstoff des seidenspinners, IV. Die synthese des bombykols und der cis-trans-isomeren hexadecadien-(10.12)-ole-(1). *Justus Liebigs Ann. Chem.* 658, 39–64.
- Byer, J.A., 2006. Pheromone component patterns of moth evolution revealed by computer analysis of the Pherolist. *J. Anim. Ecol.* 75, 399–407.
- Cardé, R.T., Cardé, A.M., Hill, A.S., Roelofs, W.L., 1977. Sex pheromone specificity as a reproductive isolating mechanism among the sibling species *Archips argyrospilus* and *A. mortuana* and other sympatric tortricine moths (Lepidoptera: tortricidae). *J. Chem. Ecol.* 3, 71–84.
- Cardé, R.T., Haynes, K.F., 2004. Structure of the pheromone communication channel in moths. In: Cardé, R.T., Millar, J.G. (Eds.), Advances in Insect Chemical Ecology. Cambridge University Press, Cambridge, pp. 283–332.
- Carlsson, M.A., Galizia, C.G., Hansson, B.S., 2002. Spatial representation of odours in the antennal lobe of the moth *Spodoptera littoralis* (Lepidoptera: Noctuidae). *Chem. Senses* 27, 231–244.
- Chang, X.Q., Nie, X.P., Zhang, Z., Zeng, F.F., Lv, L., Zhang, S., Wang, M.Q., 2017. De novo analysis of the oriental armyworm *Mythimna separata* antennal transcriptome and expression patterns of odorant-binding proteins. *Comp. Biochem. Physiol. Part D* 22, 120–130.
- Chang, X.Q., Zhang, S., Lv, L., Wang, M.Q., 2015. Insight into the ultrastructure of antennal sensilla of *Mythimna separata* (Lepidoptera: Noctuidae). *J. Insect Sci.* 15 (1), 124.
- Chang, H., Guo, M., Wang, B., Liu, Y., Dong, S., Wang, G., 2016. Sensillar expression and responses of olfactory receptors reveal different peripheral coding in two *Helicoverpa* species using the same pheromone components. *Sci. Rep.* 6, 18742.
- Chang, H., Liu, Y., Ai, D., Jiang, X., Dong, S., Wang, G., 2017. A pheromone antagonist regulates optimal mating time in the moth *Helicoverpa armigera*. *Curr. Biol.* 27, 1610–1615.
- Christensen, T.A., Mustaparta, H., Hildebrand, J.G., 1995. Chemical communication in heliothine moths VI. Parallel pathways for information processing in the macroglomerular complex of the male tobacco budworm moth *Heliothis virescens*. *J. Comp. Physiol.* 177, 545–557.
- Cork, A., Boo, K.S., Dunkelblum, E., Hall, D.R., Jee-Rajunga, K., Kehat, M., Kong Jie, E., Park, K.C., Tepgidagarn, P., Xun, L., 1992. Female sex pheromone of oriental tobacco budworm, *Helicoverpa assulta* (Guenee) (Lepidoptera: Noctuidae): Identification and field testing. *J. Chem. Ecol.* 18 (3), 403–418.

- de Fouchier, A., Walker III, W.B., Montagné, N., Steiner, C., Binyameen, M., Schlyter, F., et al., 2017. Functional evolution of Lepidoptera olfactory receptors revealed by deorphanization of a moth repertoire. *Nat. Commun.* 8, 15709.
- Du, L., Zhao, X., Liang, X., Gao, X., Liu, Y., Wang, G., 2018. Identification of candidate chemosensory genes in *Mythimna separata* by transcriptomic analysis. *BMC Genom.* 19, 518.
- Dunkelblum, E., Kehat, M., 1989. Female sex pheromone components of *Heliothis peltigera* (Lepidoptera: Noctuidae) chemical identification from gland extracts and male response. *J. Chem. Ecol.* 15 (8), 2233–2244.
- Fishilevich, E., Vosshall, L.B., 2005. Genetic and functional subdivision of the *Drosophila* antennal lobe. *Curr. Biol.* 15 (17), 1548–1553.
- Fleischer, J., Pregitzer, P., Breer, H., Krieger, J., 2018. Access to the odor world: olfactory receptors and their role for signal transduction in insects. *Cell. Mol. Life Sci.* 75, 485–508.
- Galizia, C.G., Sachse, S., Mustaparta, H., 2000. Calcium responses to pheromones and plant odors in the antennal lobe of the male and female moth *Heliothis virescens*. *J. Comp. Physiol.* 186, 1049–1063.
- Gothilf, S., Kehat, M., Jacobson, M., Galun, R., 1978. Sex attractants for male *Heliothis armigera* (Hbn.). *Experientia* 34, 853–854.
- Grosse-Wilde, E., Gohl, T., Bouche, E., Breer, H., Krieger, J., 2007. Candidate pheromone receptors provide the basis for the response of distinct antennal neurons to pheromonal compounds. *Eur. J. Neurosci.* 25, 2364–2373.
- Hansson, B.S., Almaas, T.J., Anton, S., 1995. Chemical communication in heliothine moths V. Antennal lobe projection patterns of pheromone-detecting olfactory receptor neurons in the male *Heliothis virescens* (Lepidoptera: Noctuidae). *J. Comp. Physiol.* 177, 535–543.
- Hansson, B.S., Anton, S., 2000. Function and morphology of the antennal lobe: new developments. *Annu. Rev. Entomol.* 45, 203–231.
- Hansson, B.S., Christensen, T.A., Hildebrand, J.G., 1991. Functionally distinct subdivisions of the macroglomerular complex in the antennal lobe of the male sphinx moth *Manduca sexta*. *J. Comp. Neurol.* 312, 264–278.
- Hansson, B.S., Ljungberg, H., Hallberg, E., Löfstedt, C., 1992. Functional specialization of olfactory glomeruli in a moth. *Science* 256, 1313–1315.
- Hansson, B.S., Stensmyr, M.C., 2011. Evolution of insect olfaction. *Neuron* 72, 698–711.
- He, Y.Q., Feng, B., Guo, Q.S., Du, Y., 2017. Age influences the olfactory profiles of the migratory oriental armyworm *Mythimna separata* at the molecular level. *BMC Genom.* 18, 32.
- Hildebrand, J.G., Shepherd, G.M., 1997. Mechanisms of olfactory discrimination: converging evidence for common principles across phyla. *Annu. Rev. Neurosci.* 20, 595–631.
- Hillier, N.K., Baker, T.C., 2016. Pheromones of heliothine moths. In: Allison, J.D., Cardé, R.T. (Eds.), *Pheromone Communication in Moths: Evolution, Behavior, and Application*. University of California Press, Oakland, California, pp. 301–333.
- Jiang, N.J., Tang, R., Wu, H., Xu, M., Ning, C., Huang, L.Q., Wang, C.Z., 2019. Dissecting sex pheromone communication of *Mythimna separata* (Walker) in North China from receptor molecules and antennal lobes to behavior. *Insect Biochem. Mol. Biol.* 111, 103176.
- Jiang, X.J., Guo, H., Di, C., Yu, S., Zhu, L., Huang, L.Q., Wang, C.Z., 2014. Sequence similarity and functional comparisons of pheromone receptor orthologs in two closely related *Helicoverpa* species. *Insect Biochem. Mol. Biol.* 48, 63–74.
- Kehat, M., Gothilf, S., Dunkelblum, E., Greenberg, S., 1980. Field evaluation of female sex pheromone components of the cotton bollworm, *Heliothis armigera*. *Entomol Exp Appl* 27, 188–193.
- Kennedy, J.S., 1978. The concept of olfactory ‘arrestment’ and ‘attraction’. *Physiol. Entomol.* 3, 91–98.
- Klun, J.A., Bierl-Leonhardt, B.A., Plimmer, J.R., Sparks, A.N., Primiani, M., Chapman, O. L., Lepone, G., Lee, G.H., 1980. Sex pheromone chemistry of the female tobacco budworm moth, *Heliothis virescens*. *J. Chem. Ecol.* 6, 177–183.
- Krieger, J., Grosse-Wilde, E., Gohl, T., Dewer, Y.M., Raming, K., Breer, H., 2004. Genes encoding candidate pheromone receptors in a moth (*Heliothis virescens*). *Proc. Natl. Acad. Sci. U.S.A.* 101, 11845–11850.
- Leal, W.S., 2013. Odorant reception in insects: roles of receptors, binding proteins, and degrading enzymes. *Annu. Rev. Entomol.* 58, 373–391.
- Lee, S.G., Carlsson, M.A., Hansson, B.S., Todd, J.L., Baker, T.C., 2006. Antennal lobe projection destinations of *Helicoverpa zea* male olfactory receptor neurons responsive to heliothine sex pheromone components. *J. Comp. Physiol.* 192, 351–363.
- Li, R.T., Huang, L.Q., Wang, C.Z., 2020. A moth odorant receptor highly expressed in the ovipositor is involved in detecting host-plant volatiles. *eLife*, e53706.
- Liu, Y., Liu, C., Lin, K., Wang, G., 2013. Functional specificity of sex pheromone receptors in the cotton bollworm *Helicoverpa armigera*. *PLoS One* 8, e62094.
- Liu, X.L., Sun, S.J., Khuhro, S.A., Elzaki, M.E.A., Yan, Q., Dong, S.L., 2019. Functional characterization of pheromone receptors in the moth *Aethes dissimilis* (Lepidoptera: Noctuidae). *Pestic. Biochem. Physiol.* 158, 69–76.
- Liu, Z., Wang, X., Lei, C., Zhu, F., 2017. Sensory genes identification with head transcriptome of the migratory armyworm *Mythimna separata*. *Sci. Rep.* 7, 46033.
- Löfstedt, C., 1993. Moth pheromone genetics and evolution. *Philos. T. R. Soc. B* 340, 167–177.
- Löfstedt, C., Herrebout, W.M., Menken, S.B.J., 1991. Sex pheromones and their potential role in the evolution of reproductive isolation in small ermine moths (Yponomeutidae). *Chemoecology* 2, 20–28.
- Löfstedt, C., van der Pers, J.N., 1985. Sex pheromones and reproductive isolation in four european small ermine moths. *J. Chem. Ecol.* 11, 649–666.
- McDonough, L.M., Davis, H.G., Chapman, P.S., Smithhisler, C.L., 1995. Codling moth, *Cydia pomonella*, (Lepidoptera: tortricidae): is its sex pheromone multicomponent? *J. Chem. Ecol.* 21, 1065–1071.
- Mitsuno, H., Sakurai, T., Murai, M., Yasuda, T., Kugimiya, S., Ozawa, R., Toyohara, H., Takabayashi, J., Miyoshi, H., Nishioka, T., 2008. Identification of receptors of main sex-pheromone components of three Lepidopteran species. *Eur. J. Neurosci.* 28 (5), 893–902.
- Montagné, N., Chertemps, T., Brigaud, I., Francois, A., Francois, M.C., de Fouchier, A., Lucas, P., Larsson, M.C., Jacquin-Joly, E., 2012. Functional characterization of a sex pheromone receptor in the pest moth *Spodoptera littoralis* by heterologous expression in *Drosophila*. *Eur. J. Neurosci.* 36 (5), 2588–2596.
- Nesbitt, B.F., Beevor, P.S., Hall, D.R., Lester, R., 1979. Female sex pheromone components of the cotton bollworm, *Heliothis armigera*. *J. Insect Physiol.* 25, 535–541.
- Ochieng, S.A., Anderson, P., Hansson, B.S., 1995. Antennal lobe projection patterns of olfactory receptor neurons involved in sex pheromone detection in *Spodoptera littoralis* (Lepidoptera: Noctuidae). *Tissue Cell* 27 (2), 221–232.
- Roelofs, W.L., Hill, A.S., Cardé, R.T., Baker, T.C., 1974. Two sex pheromone components of the tobacco budworm moth *Heliothis virescens*. *Life Sci.* 14, 1555–1562.
- Rothschild, G.H.L., 1978. Attractants for *Heliothis armigera* and *Heliothis punctigera*. *J. Aust. Entomol. Soc.* 17, 389–390.
- Rothschild, G.H.L., Nesbitt, B.F., Beevor, P.S., Cork, A., Hall, D.R., Vickers, R.A., 1982. Studies of the female sex pheromone of the native budworm, *heliothis punctiger*. *Entomol. Exp. Et Appl.* 31 (4), 395–401.
- Shaver, T.N., Lopez, J.D., Harstack, A.W., 1982. Effects of pheromone components and their degradation products on the response of *Heliothis* spp to traps. *J. Chem. Ecol.* 8, 755–762.
- Simossis, V.A., Heringa, J., 2003. The PRALINE online server: optimising progressive multiple alignment on the web. *Comput. Biol. Chem.* 27 (4–5), 511–519.
- Simossis, V.A., Heringa, J., 2005. PRALINE: a multiple sequence alignment toolbox that integrates homology-extended and secondary structure information. *Nucleic Acids Res.* 33, W289–W294.
- Tamura, K., Stecher, G., Peterson, D., Filipski, A., Kumar, S., 2013. MEGA6: molecular evolutionary genetics analysis version 6.0. *Mol. Biol. Evol.* 30 (12), 2725–2729.
- Tang, R., Jiang, N.J., Ning, C., Li, G.C., Huang, L.Q., Wang, C.Z., 2020. The olfactory reception of acetic acid and ionotropic receptors in the Oriental armyworm, *Mythimna separata* Walker. *Insect Biochem. Mol. Biol.* 118 (103312).
- Teal, P.E., Heath, R.R., Tumlinson, J.H., McLaughlin, J.R., 1981. Identification of a sex pheromone of *Heliothis subflexa* (GN.) (Lepidoptera: Noctuidae) and field trapping studies using different blends of components. *J. Chem. Ecol.* 7, 1011–1022.
- Touhara, K., Vosshall, L.B., 2009. Sensing odors and pheromones with chemosensory receptors. *Annu. Rev. Physiol.* 71, 307–332.
- Tumlinson, J.H., Hendricks, D.E., Mitchell, E.R., Doolittle, R.E., Brennan, M.M., 1975. Isolation, identification, and synthesis of the sex pheromone of the tobacco budworm. *J. Chem. Ecol.* 1, 203–214.
- Vickers, N.J., Christensen, T.A., Hildebrand, J.G., 1998. Combinatorial odor discrimination in the brain: attractive and antagonist odor blends are represented in distinct combinations of uniquely identifiable glomeruli. *J. Comp. Neurol.* 400, 35–56.
- Vickers, N.J., Christensen, T.A., Mustaparta, H., Baker, T.C., 1991. Chemical communication in heliothine moths III. Flight behavior of male *Helicoverpa zea* and *Heliothis virescens* in response to varying ratios of intraspecific and interspecific sex pheromone components. *J. Comp. Physiol.* A. 169, 275–280.
- Wang, G., Vasquez, G.M., Schal, C., Zwiebel, L.J., Gould, F., 2011. Functional characterization of pheromone receptors in the tobacco budworm *Heliothis virescens*. *Insect Mol. Biol.* 20, 125–133.
- Wang, H.L., Zhao, C.H., Wang, C.Z., 2005. Comparative study of sex pheromone composition and biosynthesis in *Helicoverpa armigera*, *H. assulta* and their hybrid. *Insect Biochem. Mol. Biol.* 35, 575–583.
- Witzgall, P., Stelinski, L., Gut, L., Thomson, D., 2008. Codling moth management and chemical ecology. *Annu. Rev. Entomol.* 53, 503–522.
- Wu, H., Hou, C., Huang, L.Q., Yan, F.S., Wang, C.Z., 2013. Peripheral coding of sex pheromone blends with reverse ratios in two *Helicoverpa* species. *PloS One* 8, e70078.
- Wu, H., Xu, M., Hou, C., Huang, L.Q., Dong, J.F., Wang, C.Z., 2015. Specific olfactory neurons and glomeruli are associated to differences in behavioral responses to pheromone components between two *Helicoverpa* species. *Front. Behav. Neurosci.* 9, 206.
- Wyatt, T.D., 2014. Pheromones and Animal Behavior: Chemical Signals and Signatures, second ed. Cambridge University Press, Cambridge.
- Xu, M., Dong, J.F., Wu, H., Zhao, X.C., Huang, L.Q., Wang, C.Z., 2017. The inheritance of the pheromone sensory system in two *Helicoverpa* species: dominance of *H. armigera* and possible introgression from *H. assulta*. *Front. Cell. Neurosci.* 10, 302.
- Xu, M., Guo, H., Hou, C., Wu, H., Huang, L.Q., Wang, C.Z., 2016. Olfactory perception and behavioral effects of sex pheromone gland components in *Helicoverpa armigera* and *Helicoverpa assulta*. *Sci. Rep.* 6, 22998.
- Yang, K., Huang, L.Q., Ning, C., Wang, C.Z., 2017. Two single-point mutations shift the ligand selectivity of a pheromone receptor between two closely related moth species. *eLife*, e29100.
- Zhang, D.D., Löfstedt, C., 2013. Functional evolution of a multigene family: orthologous and paralogous pheromone receptor genes in the turnip moth, *Agrotis segetum*. *PloS One* 8 (10), e77345.
- Zhang, D.D., Zhu, K.Y., Wang, C.Z., 2010. Sequencing and characterization of six cDNAs putatively encoding three pairs of pheromone receptors in two sibling species, *Helicoverpa armigera* and *Helicoverpa assulta*. *J. Insect Physiol.* 56, 586–593.

- Zhang, J.P., Salcedo, C., Fang, Y.L., Zhang, R.J., Zhang, Z.N., 2012. An overlooked component: (Z)-9-tetradecenal as a sex pheromone in *Helicoverpa armigera*. *J. Insect Physiol.* 58, 1209–1216.
- Zhang, Y.N., Du, L.X., Xu, J.W., Wang, B., Zhang, X.Q., Yan, Q., Wang, G., 2019. Functional characterization of four sex pheromone receptors in the newly discovered maize pest *Athetis lepigone*. *J. Insect Physiol.* 113, 59–66.
- Zhang, Y.N., Zhang, J., Yan, S.W., Chang, H.T., Liu, Y., Wang, G.R., Dong, S.L., 2014. Functional characterization of sex pheromone receptors in the purple stem borer, *Sesamia inferens* (Walker). *Insect Mol. Biol.* 23 (5), 611–620.